A new balaenopterid species from the Southern North Sea Basin informs about phylogeny and taxonomy of *Burtinopsis* and *Protororqualus* (Cetacea, Mysticeti, Balaenopteridae)

Michelangelo Bisconti[1,2] and Mark E.J. Bosselaers[3]

[1] Dipartimento di Scienze della Terra, Università degli studi di Torino, Torino, Italia
[2] Paleobiology Department, San Diego Natural History Museum, San Diego, CA, USA
[3] Royal Belgian Institute of Natural Sciences, Brussels, Belgium

Corresponding author
Michelangelo Bisconti, michelangelo.bisconti@unito.it

ABSTRACT

Background: An extensive radiation can be inferred among balaenopterid mysticetes in the last 10 million years based on a rich fossil record. Many extinct genera and species have been established in the past by the study of fossil rorquals from northern and southern hemispheres. In many cases, the new fossils are used to create new genera. However, in very recent times, new species of known genera have been described that help our understanding of the speciation processes and the biogeography of these whales. Here, a new species of balaenopterid whales is described in order to better understand the past diversity of Balaenopteridae and to analyze its paleobiogeographical implications. As the new species closely resembles a taxon established in the 19th century (i.e., *Burtinopsis*), a detailed analysis of this taxon was necessary to support the new taxonomic statements of this article.
Methods: A new partial skeleton including skull and earbones is described and compared to an extended sample of living and fossil mysticete species. A phylogenetic analysis including 355 character states scored in 88 taxa was performed to understand its relationships within the genus *Protororqualus*, to allow paleobiogeographic inferences and to better understand the relationships of *Protororqualus* within Balaenopteridae. Maximum parsimony analyses of character evolution were performed to understand morphological transformations within Balaenopteridae. The revision of *Burtinopsis* was carried out based on detailed descriptions and comparisons of the type materials that were figured and measured.
Results: *Protororqualus wilfriedneesi* sp. nov. was established based on a comparative analysis of the skull and earbone morphology. The specimen is dated back to the Zanclean (Lower Pliocene, between *c.* 5.3 and 3.6 Ma). A taphonomical study of the holotype skeleton revealed evidence of interactions with sharks and fishes before the definitive burial of the carcass. Based on the phylogenetic analysis, the monophyly of the genus *Protororqualus* was confirmed. *Protororqualus wilfriedneesi* sp. nov. was more derived than *Protororqualus cuvieri* suggesting that it resulted from an invasion of the North Sea Basin (and the North Atlantic ocean) from the Mediterranean basin. Several specimens from western and eastern sides of the

Atlantic Ocean are described that suggest that *Protororqualus wilfriedneesi* had a trans-Atlantic distribution in the Pliocene.

INTRODUCTION

The genus *Protororqualus* was established by *Bisconti (2007a)* based on an almost complete skeleton from Mount Pulgnasco, a locality at a short distance from Parma (Northern Italy). That skeleton included the skull, both dentaries and most of the postcranial bones, and was the subject of a number of descriptions including those of *Cortesi (1819)* and *Cuvier (1823)*. *Van Beneden (1875)* provided a new assessment of the specimen based on the photographic plates provided by Prof. Emilio Cornalia who, at the time, was the director of the natural history museum of Milan. The specimen was certainly the most famous mysticete skeleton in Italy because, at that time, it was the most complete mysticete fossil of Europe. *Bisconti (2009, 2007a)* detailed the taxonomic debate concerning that specimen and mentioned the fact that the skeleton from Mount Pulgnasco was destroyed due to a bombing run over Milano during the Second World War. A 3D reconstruction of this lost specimen is currently on exhibit at the Museo Geopaleontologico *Giuseppe Cortesi* in Castell'Arquato, Northern Italy (*Bisconti & Francou, 2014*).

The Mount Pulgnasco skeleton assumed noteworthy importance since *Zeigler, Chan & Barnes (1997)* suggested that it represents a stem-balaenopterid taxon retaining archaic morphological characters in the skull. For this reason, the surviving evidence about this specimen was reviewed and re-analyzed by *Bisconti (2007a)* leading to the creation of the new combination *Protororqualus cuvieri* that was then used by a number of students in assessing the phylogenetic relationships of Balaenopteridae (see below for a detailed discussion on this point with citations of the appropriate references).

The continuous discoveries of fossil mysticetes from construction sites and research cruises along the Scheldt River at different localities in Belgium and Holland brought to light a wealth of new mysticete taxa including balaenopterids such as *Nehalaennia devossi* (*Bisconti, Munsterman & Post, 2019*), *Archaebalaenoptera liesselensis* (*Bisconti et al., 2020*), *Fragilicetus velponi* (*Bisconti & Bosselaers, 2016*), cetotheriids such as *Metopocetus hunteri* (*Marx, Bosselaers & Louwye, 2016*), *Herentalia* nigra (*Bisconti, 2015*) and *Tranatocetus maregermanicum* (*Marx et al., 2019*), and basal thalassotherian species such as *Parietobalaena campiniana* (*Bisconti, Lambert & Bosselaers, 2013*). In specific cases, these new discoveries permitted the revision of taxa that Van Beneden established in the 19th century in a way that is currently considered methodologically inadequate (*Deméré, Berta & McGowen, 2005*; *Bisconti, Lambert & Bosselaers, 2013*; *Bisconti, Lambert & Bosselaers, 2017*; *Bosselaers & Post, 2010*; *Steeman, 2010*).

In the present article, we describe a new mysticete discovered at a locality close to the city of Antwerp (Flanders, Belgium). The preserved portions include a partial skull with earbones and very partial postcrania. The specimen is currently held by the Royal Belgian Institute of Natural Sciences (hereinafter, RBINS) with the accession number M 2315. A comparative analysis of the specimen revealed that it represents a new species of *Protororqualus* and the anatomical portions preserved allowed a new phylogenetic analysis of Balaenopteridae in the broader framework of chaeomysticete phylogenetics providing a new and well-resolved branching pattern for the whole suborder Mysticeti.

Interestingly, the earbone morphology is close to some of the specimens that *Van Beneden (1882)* assigned to the genus *Burtinopsis* and, for this reason, in this paper we make a taxonomic revision of this genus based on a new examination of all the type materials and a specimen-by-specimen comparative analysis.

Based on our new study of *Burtinopsis* and *Protororqualus*, here, we provide new taxonomic decisions and phylogenetic interpretations for Balaenopteridae and the whole Mysticeti clade.

MATERIALS AND METHODS

Materials

The new species is based on a partial skull and associated postcrania held by RBINS with the number M2315. Materials belonging to the RBINS Van Beneden type collection that have been previously assigned to *Burtinopsis* species include specimens M 682–685, 691–694, 696–709, and 800 (Fig. 1).

Comparative anatomy and terminology

Anatomical terminology for the skull and petrotympanic complex is based on *Mead & Fordyce (2009)* and, when necessary, *Ekdale, Berta & Deméré (2011)* and *Kellogg (1965, 1968)*. The anatomical terminology for the postcranial skeleton is based on *Martìnez-Cáceres, Lambert & De Muizon (2017)*, *Schaller (1999)*, *Nickel, Schummer & Seiferle (1991)* and *Gray (1977)*. The following abbreviations are used throughout the text: C, cervical vertebra; Cd, caudal vertebra; L, lumbar vertebra; T, thoracic vertebra. Anatomical abbreviations used in the illustrations are the following: anl, anterior lip; antp, anterior pedicle of petrotympanic; ap, anterior process of periotic; aplp, lateral tuberosity of periotic; asc max, ascending process of maxilla; bc-bs, basioccipital-basisphenoid suture; bcr, basicranium; bop, basioccipital; bs-pt, basisphenoid-pterygoid suture; cop, conical process; crh, cranial hiatus; ctpp, caudal tympanic process of promontorium; dia, diaphysys; eam, external acoustic meatus; elf, endolymphatic foramen; epi, epiphysis or articular head of humerus; euo, Eustachian opening; exo, exoccipital; fm, foramen magnum; fon, fontanella; for, dorsal infraorbital foramen; fr, frontal; fr-ma, frontal-maxilla suture; fr-pa, frontal-parietal suture; grt, greater tubercle; inb, involucral bulge; inr, involucral ridge; inv, involucrum; jno, jugular notch; lpc, lateral prominence; MAI, internal acoustic meatus; malf, fossa for malleus; mar, main ridge; mat, mallear attachment point; max, maxilla; oc, occipital condyle; op, optic canal; ow, oval window; par, parietal; pa-fr, parietal-frontal suture; pal, palatine; pa-pa, interparietal suture;
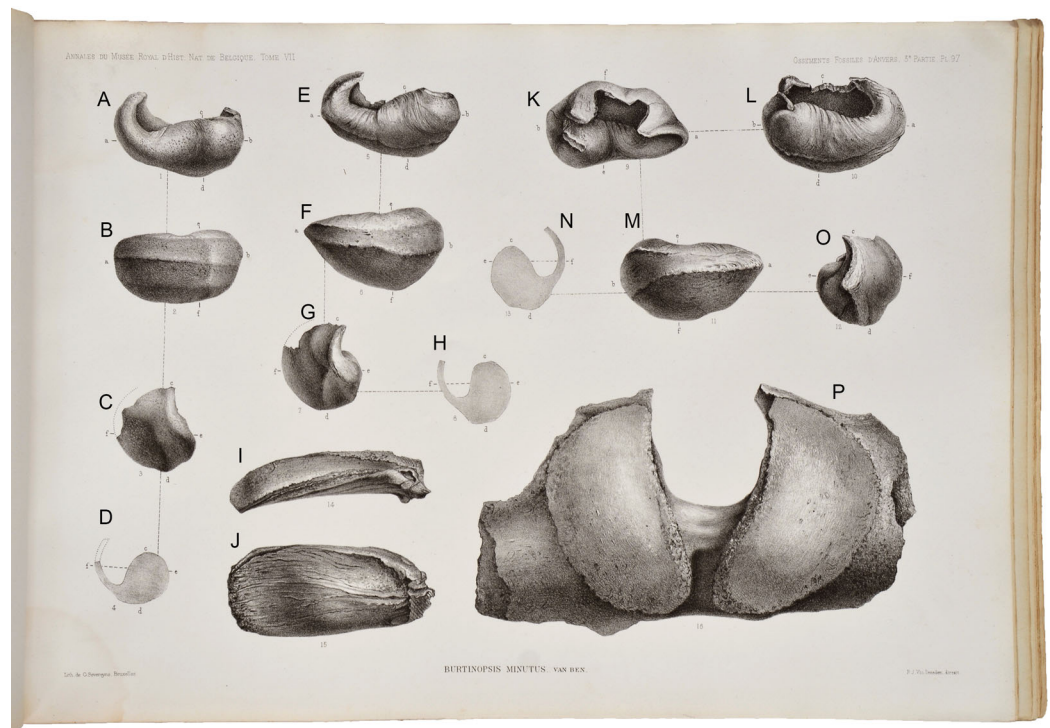
Figure 1 Early representation of *Burtinopsis*. Representation of Burtinopsis in the monumental atlas realized under the direction of *Van Beneden (1882)*. Specimen M 700 in (A) medial view; (B) ventral view; (C) posterior view; (D) cross-section. Specimen M 701 in (E) medial view; (F) ventral view; (G) posterior view; (H) cross-section. Specimen M 699 in (I) anteroventral view; (J) dorsal view. Specimen M 702 in (K) dorsal view; (L) medial view; (M) ventral view; (N) cross-section; (O) anterior view. Specimen M 698 in (P) posterior view.

pa-sq, parietal-squamosal suture; pgl, postglenoid process of squamosal; plf, perilymphatic foramen; pl-pt, palatine-pterygoid suture; pof, pseudoval fossa; posp, posterior pedicle of petrotympanic; pp, dorsal portion of periotic; pp-ex, posterior process of periotic-exoccipital contact; ppp, posterior process of the periotic; pp-sq, posterior process of periotic-squamosal articulation; prgr, promontorial groove; prom, promontorium (pars cochlearis); pso, foramen pseudo-ovale; pte, pterygoid; ptf, pterygoid fossa; pt-fr, pterygoid-frontal contact; pt-sq, pterygoid-squamosal suture; rw, round window; sip, sigmoid process; soc, supraoccipital; soe, anterior supraorbital edge; sq, squamosal; stmf, stylomastoid fossa; ttmc, tensor tympani muscle condyct; tyc, tympanic cavity; vel, anterolateral expansion (anterior lobe); VII-c, endocranial opening of facial canal.

Taphonomy

The bones of the new balaenopterid skeleton were mapped as they were exposed during excavation. Associated shells and barnacles were observed and collected at the discovery site allowing for paleoecological and paleoenvironmental interpretations. Bite marks generated by interactions with fishes or sharks were counted, photographed and measured for interpretation.

Nomenclatural act

The electronic version of this article in Portable Document Format (PDF) will represent a published work according to the International Commission on Zoological Nomenclature (ICZN), and hence the new names contained in the electronic version are effectively published under that Code from the electronic edition alone. This published work and the nomenclatural acts it contains have been registered in ZooBank, the online registration system for the ICZN. The ZooBank LSIDs (Life Science Identifiers) can be resolved and the associated information viewed through any standard web browser by appending the LSID to the prefix http://zoobank.org/. The LSIDs for this publication is: urn:lsid: zoobank.org:pub:0E5931ED-C1B7-44D5-BBB4-0A74C9A06A55. The online version of this work is archived and available from the following digital repositories: PeerJ, PubMed Central and CLOCKSS.

Phylogenetic analysis

The phylogenetic analysis was carried out based on a morphological dataset including 355 characters from osteology and baleen morphology scored for 88 taxa based on the dataset provided *Bisconti et al. (2020)* that is, in its turn, a modification of the dataset of *Bisconti, Munsterman & Post (2019)*. The taxonomic sample included representatives of all the mysticete radiations and 35 nominal balaenopterid species. A commented character list and the matrix used for phylogenetic analysis are provided in the Supplemental Information. The matrix was treated in TNT 1.5 (*Goloboff & Catalano, 2016*) by holding a treespace of 20000 cladograms in the tree buffer and performing 2000 replications of Tree Bisection Reconnection algorithm (TNT command mult 2000 = tbr) retaining 10 trees each. Protocetidae was set as outgroup. An analysis using implied weights (default parameters: function $k = 3.0$) was also performed by using all the new technology algorithms as implemented in TNT and hitting the shortest trees 10 times at least. Then a traditional search was done based on the trees stored in the RAM. The available RAM was 16 MB with 6% occupied by the buffer. The total memory required for the data was 0.56 MB. Node support was calculated in TNT by bootstrap (1,000 replicates, traditional search with default parameters), symmetric resampling (1,000 replicates, absolute frequencies) and Bremer support (suboptimal value set to 10). Character mappings onto the preferred cladograms were performed through MESQUITE 3.6 (*Maddison & Maddison, 2019*).

RESULTS: TAXONOMIC REVISION OF *BURTINOPSIS*

Van Beneden established two species of *Burtinopsis*, namely *B. minutus* (RBINS M 696-709), *B. similis* (RBINS M 682-689, 691-694, 800), based on remains coming from different localities (Table 1). *Burtinopsis similis* is represented by 14 inventoried specimens whose labels indicate they belong to 12 different individuals at least. *Burtinopsis minutus* is represented by 14 inventoried specimens whose labels suggest they belong to 12 different individuals at least. The individuals assigned to both these species by *Van Beneden (1882)* are mostly represented by disparate anatomical portions that make it extremely hard-to-impossible to group them together. All the specimens that were

Table 1 Materials previously assigned to *Burtinopsis* by *Van Beneden (1882)*. Materials assigned to Burtinopsis by *Van Beneden (1882)* including data from the museum labels available from RBINS. Data include: (1) repository number; (2) original taxonomic assignment by Van Beneden; (3) anatomical portion; (4) provenance; (5) original stratigraphic position; (6) new stratigraphic assessment (this work); and (7) new taxonomic decision (this work).

Repository number	Original taxonomy	Anatomical portion[1]	Locality	Original age	Revised age	New taxonomic decision
M 682a–c	*Burtinopsis similis*	pC2, 3 pC indet.	Bassin du Nord d'Anvers	Scaldisien	L Zancl.-E Piac.	Thalassotherii indet.
M 683a–b	*Burtinopsis similis*	pS, pM(ls)	Antwerp, 3rd st	Scaldisien	L Zancl.-E Piac.	Thalassotherii indet.
M 684	*Burtinopsis similis*	pM(rs)		Scaldisien	L Zancl.-E Piac.	Balaenopteridae indet.
M 685	*Burtinopsis similis*	pM(ls)	Antwerp, 2nd ?st	Scaldisien	L Zancl.-E Piac.	Balaenopteridae indet.
M 686	*Burtinopsis similis*	pB(ls)	?Antwerp	Scaldisien	L Zancl.-E Piac.	Balaenopteridae indet.
M 687	*Burtinopsis similis*	pB(ls)	?Antwerp	Scaldisien	L Zancl.-E Piac.	Balaenopteridae indet.
M 688	*Burtinopsis similis*	pB(ls)	?Antwerp	Scaldisien	L Zancl.-E Piac.	*Protororqualus wilfriedneesi*
M 689	*Burtinopsis similis*	C1	Antwerp, fort 3, Borsbeck	Scaldisien	L Zancl.-E Piac.	Balaenomorpha indet.
M 691	*Burtinopsis similis*	Cd indet.	Antwerp, 2nd st, Stuyvenberg	Scaldisien	L Zancl.-E Piac.	Balaenomorpha indet.
M 692	*Burtinopsis similis*	Cd indet.	Antwerp, Stuyvenberg	Scaldisien	L Zancl.-E Piac.	Balaenomorpha indet.
M 693	*Burtinopsis similis*	H(ls)	Antwerp, fort 3	Scaldisien	L Zancl.-E Piac.	Thalassotherii indet.
M 694	*Burtinopsis similis*	U(ls)	Antwerp, 2nd st, Stuyvenberg	Scaldisien	L Zancl.-E Piac.	Balaenomorpha indet.
M 695	*Burtinopsis similis*	R(ls)	Antwerp, Bassin du Nord	Scaldisien	L Zancl.-E Piac.	Balaenomorpha indet.
M 696a–k	*Burtinopsis minutus*	C1, ?pC7, 6 pT indet., pL indet., 2 pCd indet.	Antwerp, 2nd st, Stuyvenberg	Scaldisien	L Zancl.-E Piac.	Thalassotherii indet.
M 697a–f	*Burtinopsis minutus*	pC2-C7, Cd indet.	Antwerp, 2nd st, Stuyvenberg	Scaldisien	L Zancl.-E Piac.	Balaenopteridae indet.
M 698	*Burtinopsis minutus*	pS	Antwerp, 2nd st, Berchem	Scaldisien	L Zancl.-E Piac.	Balaenomorpha indet.
M 699	*Burtinopsis minutus*	pPt, pS	Antwerp, Stuyvenberg	Scaldisien	L Zancl.-E Piac.	Balaenopteridae indet.
M 700	*Burtinopsis minutus*	pB(rs)	Antwerp	Scaldisien	L Zancl.-E Piac.	Balaenopteridae indet.
M 701	*Burtinopsis minutus*	pB(rs)	Antwerp, 3rd st Borgerhaut	Scaldisien	L Zancl.-E Piac.	Balaenopteridae indet.
M 702	*Burtinopsis minutus*	pB(ls)	Antwerp, fort 3, Borsbeck	Scaldisien	L Zancl.-E Piac.	*Protororqualus wilfriedneesi*
M 703	*Burtinopsis minutus*	pM(ls)	Antwerp, 2nd st	Scaldisien	L Zancl.-E Piac.	Balaenopteridae indet.
M 704	*Burtinopsis minutus*	pC1	Antwerp, 2nd st	Scaldisien	L Zancl.-E Piac.	Balaenomorpha indet.
M 705	*Burtinopsis minutus*	pC2	Antwerp, 3rd st	Scaldisien	L Zancl.-E Piac.	Thalassotherii indet.
M 706	*Burtinopsis minutus*	pSc(rs)	Antwerp	Scaldisien	L Zancl.-E Piac.	Thalassotherii indet.
M 707	*Burtinopsis minutus*	H(rs)	Antwerp	Scaldisien	L Zancl.-E Piac.	Balaenomorpha indet.
M 708	*Burtinopsis minutus*	pU(rs)	Antwerp	Scaldisien	L Zancl.-E Piac.	Balaenomorpha indet.
M 709	*Burtinopsis minutus*	R(rs)	Antwerp	Scaldisien	L Zancl.-E Piac.	Balaenomorpha indet.
M 800a–o	*Burtinopsis similis*	pC2-7, pT1-6, 2 pL indet.	Cittadelle du Nord, Auskrum	[2]		Balaenomorpha indet.

Notes:
[1] Caption: B, tympanic bulla; C, cervical vertebra; Cd, caudal vertebra; E Piac., early Piacenzian; H, humerus; L, lumbar vertebra; L Zanc., late Zanclean; ls, left; M, mandibular ramus; p, partial; Pt, periotic; R, radius; rs, right; S, skull; Sc, scapula; st., section; T, thoracic vertebra; U, ulna.
[2] Original label: L'exemplaire est exposé dans la salle I. Meuble N° 22 (Tertiaire).

previously assigned to *Burtinopsis* are labeled as Scaldisian in age. This chronostratigraphic regional unit is roughly equivalent to the Lillo Formation, a latest early-to-late Pliocene lithostratigraphic unit (latest Zanclean to Piacenzian; *Laga, Louwye & Mostaert, 2006*; *De Schepper, Head & Louwye, 2009*). The results of the specimen-by-specimen taxonomic revision of *Burtinopsis* are presented in the Supplemental Information file that is an integral part of the present article. All the specimens are figured out in Figs. S1–S54 and all the measurements are provided in the Supplemental Information file in the dedicated text and in Tables S2–S4. Based on our revision, the conclusions of which are summarized in Table 1, we recognize that 12 specimens only can be assigned to Balaenomorpha gen. et sp. indet., 7 specimens to Thalassotherii gen. et sp. indet., 9 specimens to Balaenopteridae gen. et sp. indet. and 2 specimens to cf. *Protororqualus sp.*. Based on this revision, we declare *Burtinopsis* a nomen dubium as there is not any evidence that the specimens assigned to this genus actually can form a taxonomically valid group (according with *Deméré, Berta & McGowen, 2005*). We only distinguish two specimens (RBINS M 688 and M 702), from the whole assemblage, that can be included within the same taxon but their preservation is too poor to allow a correct taxonomic use of them to establish a generic name. We, therefore, suggest that these specimens, based on their morphology, show affinities with *Protororqualus* (Table 1). Here we describe the two specimens RBINS M 688 and M 702.

RBINS M 688
Origin. ?Antwerp.

Stratigraphy. Unknown. Probably Pliocene in age.

Description. Left tympanic bulla (Fig. 2A–2E; Table S1) characterized by well developed anterolateral lobe and descending dorsal border of the involucrum. The involucral ridge is well developed and the tympanic cavity is deep with an Eustachian outlet anteriorly bordered by a low relief. The posterior border of the bulla is uniformly rounded and the conical process is comparatively high and with rounded dorsal outline. The sigmoid process is broken. The anterolateral lobe does not protrude laterally more than the posterolateral protrusion of the bulla that bears the sigmoid and the conical processes in dorsal view.

RBINS M 702
Origin. Antwerp, Fort 3, Borsbeck (Fig. S59).

Stratigraphy. A 'Scaldisian' age is suggested in the original label of the specimen. According to *Laga, Louwye & Mostaert (2006)*, this informal stage corresponds to the Lillo Formation that is late Zanclean-to-Piacenzian in age.

Description. Left tympanic bulla characterized by well developed anterolateral lobe and anteriorly descending dorsal border of the involucrum (Figs. 2F–2I). The involucral ridge is well developed and the tympanic cavity is deep (Table S1) with an Eustachian outlet anteriorly bordered by a low relief. The posterior border of the bulla is uniformly
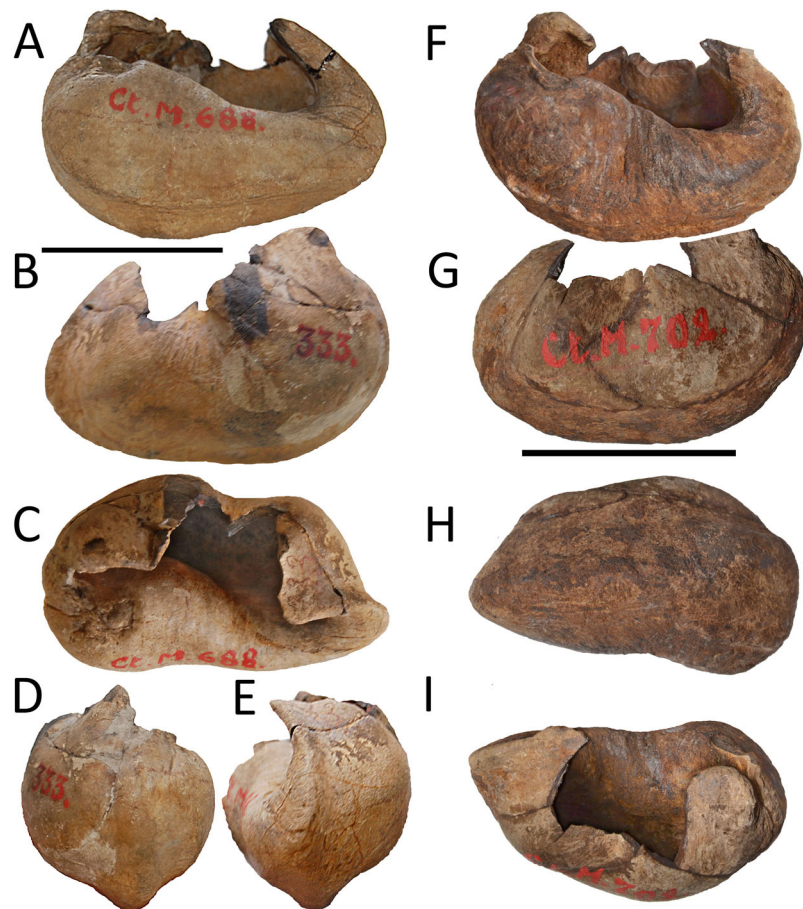
Figure 2 RBINS M688 and M702. Specimens previously assigned to Burtinopsis minutus and reassigned to cf. Protororqualus sp. in the present work. (A–E) M 688, left tympanic bulla. (A) Medial view; (B) lateral view; (C) dorsal view; (D) posterior view; (E) anterior view. (F–I) M 702, left tympanic bulla. (A) Medial view; (B) lateral view; (C) ventral view; (D) dorsal view. Scale bars equal 50 mm.

rounded. Both conical and sigmoid processes are broken. The anterolateral lobe does not protrude more laterally than the posterolateral protrusion of the bulla. Compared to RBINS M 688, this bulla is more robust and shows a higher anterior border of the tympanic cavity with more sulci on the dorsomedial surface of the involucrum.

RESULTS: A NEW BALAENOPTERID SPECIES

Systematic Paleontology

Mammalia *Linneaus, 1758*

Cetartiodactyla *Montgelard, Catzeflis & Douzery, 1997*

Cetacea *Brisson, 1762*

Pelagiceti *Uhen, 2008*

Neoceti *Fordyce & De Muizon, 2001*

Mysticeti *Cope, 1891*

Chaeomysticeti *Mitchell, 1989*

Balaenomorpha *Geisler & Sanders, 2003*
Thalassotherii *Bisconti, Lambert & Bosselaers, 2013*
Balaenopteridae *Gray, 1864*
Protororqualus *Bisconti, 2007b*

Emended diagnosis of genus. Exclusive characters: Rorqual-like exhibits a triangular and pointed anterior margin of supraoccipital (which is absent from Balaenopteridae but is present in other mysticetes), sinuous lateral edges of the supraoccipital with strong transverse compression along the anterior half of the supraoccipital, radius and ulna as long as the humerus, periotic dorsoventrally low with flat dorsal surface, scarce dorsoventral height of the pars cochlearis and mostly flat ventral surface of the pars cochlearis, anterior lobe of tympanic bulla not protruding more than the posterior portion of the lateral wall of the tympanic bulla, Eustachian outlet of tympanic bulla anteriorly bordered by a low relief, homogeneously rounded posterior outline of tympanic bulla, dorsal surface of involucrum quickly descending anteriorly in medial view; non-exclusive characters: strong attachment sites for neck muscles on the dorsolateral surface of the supraoccipital, dentary nearly straight in dorsal view.

Type species. *Protororqualus cuvieri Bisconti, 2007b*

Discussion. The type species is based on a lost specimen whose taxonomic history is detailed in *Bisconti (2007b)*. The reconstruction of the type species is based on the high-quality photographic plates provided by Emilio Cornalia to Van Beneden that were then used by Van Beneden himself in his analysis of the specimen (*Van Beneden, 1875*). A tridimensional reconstruction of the type specimen is housed at the Museo Geopaleontologico "Giuseppe Cortesi" in Castell'Arquato (Parma Province, Italy; *Bisconti & Francou, 2014*).

The type specimen was published in 1819 for the first time by Giuseppe Cortesi that described the digging operations and the provided a reconstruction of the skeleton. The earliest skeletal analyses were based on a reconstruction that was wrong in the orientation of the scapula and this led to a biased diagnosis that was subsequently corrected by *Strobel (1881)*. *Cuvier (1823)* and *Van Beneden (1875)* provided further studies on this specimen that was variously assigned to *Cetotherium*, *Plesiocetus* and *Balaenoptera* by authors like *Brandt (1873)*, *Van Beneden (1875)*, *Strobel (1881)*, *Kellogg (1931)*, *Cuscani-Politi (1961)*, *Caretto (1970)* and *Zeigler, Chan & Barnes (1997)*. *Bisconti (2007b)* reviewed the taxonomic history and the morphological evidence and concluded that: (1) there are no morphological bases for the inclusion of the specimen from Mount Pulgnasco in *Cetotherium, Plesiocetus* (based on the re-examination of the type materials that are the subject of a new paper currently in preparation by the present authors) and *Balaenoptera*, and (2) the specimen represents a new genus and species of basal balaenopterid whales. For this reason, *Bisconti (2007b)* created the genus *Protororqualus* to whom the species *P. cuvieri* (including only the specimen from Mount Pulgnasco) was assigned.

We must note that there is some confusion about the use of the terms *cuvieri* and *cuvierii* in recent literature and online databases. Most of this confusion is certainly

due to the massive synonymy made by *Caretto (1970)* within the chronospecies *Balaenoptera acutorostrata cuvierii* in which he included most of the Mysticeti records from Miocene and Pliocene of Europe. Given the monumental work done by this author, his conclusions were widely accepted by non-specialist paleontologists that assigned to this taxon a great number of fossil mysticetes from Europe. *Bisconti (2009)* outlined this problem making it evident that the chronospecies *Balaenoptera acutorostrata cuvieri* cannot be accepted because it is based on a specimen (included here in the phylogenetic analysis with the acronym UT PU13842) that does not possess the diagnostic characters of the genus *Balaenoptera* (e.g., squared posterior ends of the ascending process of the maxilla, transversely expanded anterior border of the supraoccipital, acutely triangular anterior process of the periotic, no promontorial groove in the pars cochlearis, reduced postcoronoid fossa and crest, reduced angular process of the dentary). This means that the chronospecies *Balaenoptera acutorostrata cuvierii* is a nomen dubium and must be abandoned. A new research project is being developed at the Università degli Studi di Torino (see "Acknowledgment") that focuses on the taxonomic revision and phylogenetic analysis of these problematic taxa from Northwestern Italy and we hope that this will help clarify the current taxonomic confusion.

Based on this reasoning, it is possible to assess the occurrence of *Protororqualus* specimens across Europe according to the cetacean partition of the Paleobiology Database (available at https://paleobiodb.org and mainly compiled by Mark Uhen). The data were downloaded from the Paleobiology Database on 24 April, 2020, using the taxonomic names 'Protororqualus' and 'Protororqualus cuvieri' in the search engine in two separate search runs that retrieved three records: (A) one from Italy (*Protororqualus cuvieri Bisconti, 2007b*); (B) one from The Netherlands deriving from a taxonomic list provided by *Scager et al. (2017)* without any mention of the preserved portions in the text and thus preventing eventual confirmation/rejection of the presence of this species in the areas studied by these authors; (C) one from Slovenia as published by *Pavšič & Mikuž (1996)*. The latter is represented by an articulated partial skeleton of a thalassotherian whale that the authors assigned to *Balaenoptera acutorostrata cuvierii*. A close scrutiny to the photographic plates published by *Pavšič & Mikuž (1996)* suggests that there are not enough diagnostic characters to safely assign the specimen to any known genus or species of living or fossil mysticete. Unfortunately, in fact, the skull of this specimen is heavily crushed and fragmentary thus preventing the reconstruction of diagnostic elements such as the vertex, the relationships between rostrum and frontal and the earbone morphology. For this reason, we reject the identification of the specimen cited by *Pavšič & Mikuž (1996)* and suggest that it must be classified as Thalassotherii gen. et sp. indet.

Protororqualus wilfriedneesi new species

Diagnosis of species. *Protororqualus wilfriedneesi* differs from *P. cuvieri* in having more posteriorly placed supraorbital process of the frontal with respect to the anterior end of the supraoccipital and, thus, in having an anteroposteriorly shortened temporal fossa in dorsal view.

Etymology. The species name is dedicated to Wilfried Nees who discovered the fossil.

Repository. RBINS.

Holotype. Specimen M 2315 including partial skull with both periotics (one still in articulation and one detached) and tympanic bullae, the proximal portion of a humerus and an almost complete ulna.

Horizon and locality. The specimen has been discovered on July 8th 2000, at a depth of about 3 m at a construction site near Ternesselei 164 (geographic co-ordinates: 51°12′ 27,75″ N and 4°30′25,52″E) at Wommelgem, 5 km east of Antwerp. A relatively shallow construction pit (slightly less than 5 m deep) was dug for the construction of an underground waste water basin (Fig. 3). The construction pit was dug into an outcrop of the Kattendijk Sands dating from the Early Pliocene; in fact, its age is estimated to be 5.0 to 4.4 Ma (*De Schepper, Head & Louwye, 2009*). The Kattendijk Sands occur in many locations in and around Antwerp as a distinct glauconitic sandy deposit. A peculiar pattern observed in the Kattendijk Sands Formation is called 'Post-Miocene crag' and is characterized by the presence by reddish brown clayey sand, with rather few dispersed shells and shell fragments. The skull was situated in the middle of the crag layer.

Age of the specimen. Seven shells with a restricted period of occurrence were retrieved from inside the skull during the preparation of the specimen by one of us (M. Boss, 2001, personal observations); the species found are reported in Table S4 and figured in Fig. S53. In the sediment around the skull, shells were abundant. Most of them were fractured. Many more were collected from layers above and below the specimen, further limiting stratigraphic age/horizon of the specimen. All shells examined here were collected at the site during the works by Wilfried Nees.

The seven bivalve species (*Pecten grandis*, Digitariopsis obliquata obliquata, *Laeveastarte arijanseni, Laeveastarte omalii omalii, Cardites squamulosa ampla, Pygocardia rustica tumida, Glossus humanus*; see Table S4) retrieved from within the neurocranium (Fig. S53) indicate the specimen most probably originates from the Early Pliocene Kattendijk/Luchtbal Sands. The latter is a horizon which has a patchy spatial record in the Antwerp region (*De Schepper, Head & Louwye, 2009*; p. 13; *Marquet, 2002*; *Marquet & Landau, 2006*, p.13). *Vandenberghe et al. (1998)* estimated the age of the Luchtbal Sand Member as late Zanclean, about 3.5 Ma, based on benthic foraminifer zone B11, benthic mollusk association BM22A and otholith zone 18 (*Vinken, 1988*). *De Schepper, Head & Louwye (2009)* estimated the maximum age of the Luchtbal Sand Member at 3.71 Ma and the minimum at 2.72–2.74 Ma (*De Schepper, Head & Louwye, 2009*), confining the deposit to the latest Zanclean—earliest Piacenzian (*Dewaele, Lambert & Louwye, 2018*).

The absence of *Palliolum gerardi* (*Nyst, 1835*) seems noteworthy since this species is extremely common in the late Early Pliocene Luchtbal Sand Member. The (common) occurrence of *Glossus humanus* is equally noteworthy. It occurs from the Early Pliocene till recent, but fossil specimens are especially common in the Kattendijk Sands and a common
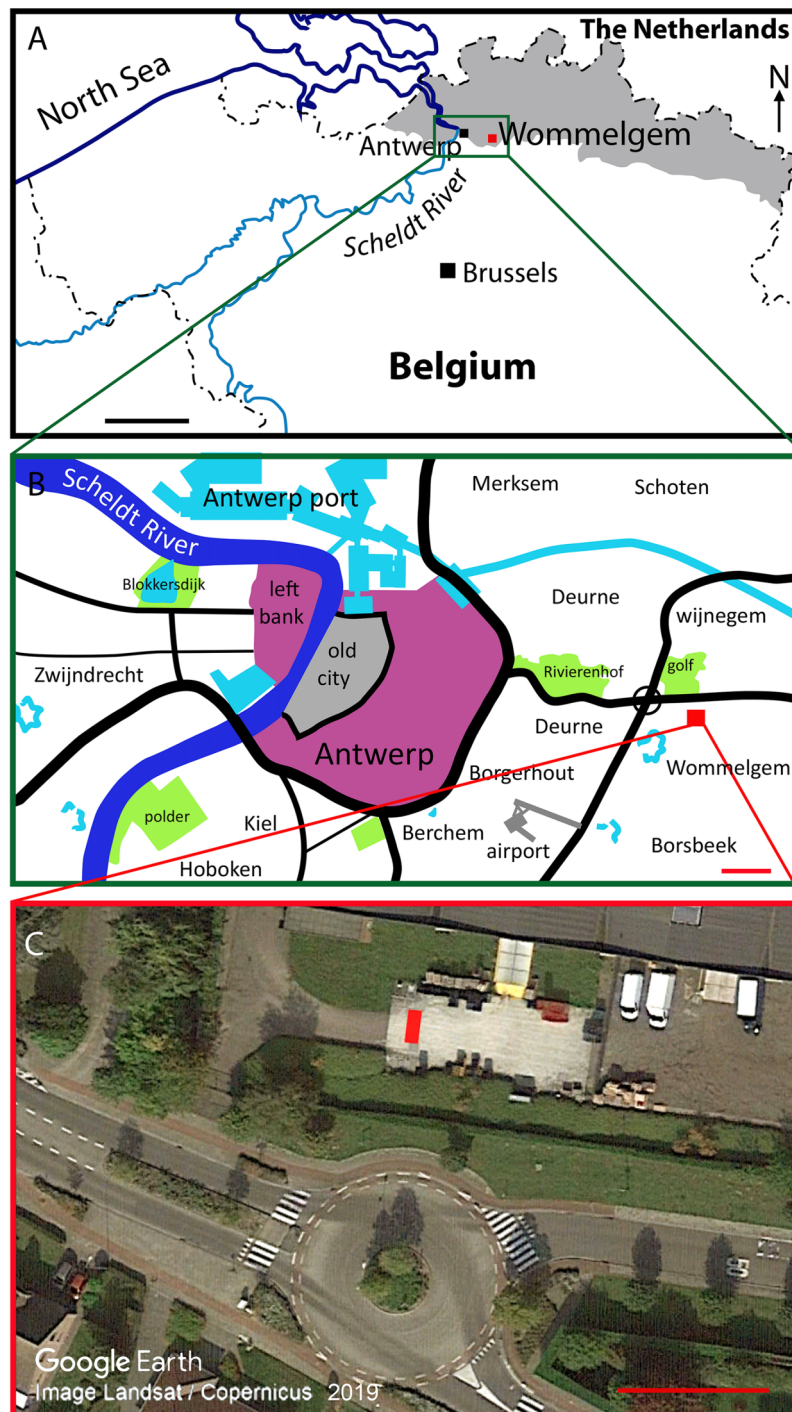
Figure 3 Discovery site of *Protororqualus wilfriedneesi* sp. nov. Site of the discovery of the holotype of Protoroqualus wilfriedneesi (RBINS M 2315). (A) Map of Belgium and adjacent countries showing the geographic position of the discovery site. (B) Map of the city of Antwerp with indication of the discovery site (red square). (C) Close-up, satellite view of the exact discovery location (red rectangle). Credits for (C): Google Earth, Landsat/Copernicus, 2019.

occurrence of this species is therefore considered a marker for this horizon (*Wesselingh & Moerdijk, 2010*; *Marquet, 2005*). The absence of *Palliolum gerardi* and the presence of *Glossus humanus* suggest that the specimen was from the Kattendijk Sands rather than the Luchtbal Sand Member. Taking all evidence into account, an Early Pliocene (Zanclean; between 5.3 and 3.6 Ma; *Louwye, Head & De Schepper, 2004*) age of this specimen is assumed.

TAPHONOMY

In general, the "post-Miocene crag" east of Antwerp (c.q., Wommelgen, Ranst, Broechem, Borsbeek, Berchem) is considered to be a homogenous mix of Pliocene shells, but the presence of lots of (mostly very) partial cetacean skeletons, preserved more or less in anatomical connection (M. Boss, 1989, 2006, 2009, 2012, 2014, personal observations; *Marquet & Herman, 2009*), makes it clear that these sediments were reworked 'mildly' and most of the original fossils were just concentrated when part of the sediment was washed away, with little or no mixing of its content (Fig. S54). Often even a layered structure is still present and can be observed in the crag deposit (M. Boss, 2000, 2001, 2009, 2013, personal observations).

Biostratinomy. As far as the current specimen is concerned, the original dispersion of the bones is partially presented in Fig. S54 where the degree of bone fragmentation is evident. Despite the heavy damage suffered by the specimen because of post-mortem processes, fragments belonging to single bones were grouped together or at short distance each other. The bones show wear probably caused by reworking. Moreover, the lack of small bone splinters (such as the missing fragments of the ventral lobes of the bullae, and the eroded edges of almost all of the bones) indicates that the specimen was exposed during a rather long time to erosive forces, including a rather strong water flow, apparently after fossilization. The fact that the skull has been found roughly in anatomical connection, including both bullae and periotics supports the hypothesis that the reworking was only "mild", but also indicates that the skeleton originally was fairly completely preserved. Both petrotympanic complexes, as well as several other bones, are fractured in centimeter-sized, cube-like fragments. This type of erosion is very typical for the Antwerp region and is most probably a result of permafrost development during the last glacial maximum, given the Mio-Pliocene fossil horizons are at a shallow depth (between 1.5 and 6 m below the surface). The dispersion of the bones of the specimen is illustrated in Fig. S54.

Palaeoecology and bite marks. In the Scheldt estuary, Early Pliocene strata were deposited in a near coastal environment with a water depth of probably less than 25 m because fossil *Balanus* species are common on Antwerp cetacean bones from the Kattendijk sands (M. Boss, 1998, 2003, 2005, 2012, personal observations). Sea surface temperatures were cool to temperate (less than 7.2 °C for April sea-surface temperatures) (*Gaemers, 1988*; *Louwye, Head & De Schepper, 2004*).

At least 5 bone fragments show a series of fine parallel scars at or near their borders (Figs. S55–S57). These scars are interpreted as post-mortem bites by small sharks or other kinds of fishes. All the bites occur on disconnected bone fragments. These bones have rather heavily bio-eroded edges and it looks like the fishes came to feed/scavenge on the

rotten bone. We could find no bites on the neurocranium that we uncovered largely in anatomical connection. This indicates the neurocranium must have been covered by sediment rather quickly after dying/decay. Some peripheral parts of the cranium were crushed and scattered around the neurocranium but for some reason they were exposed over a long time at the sea bed, allowing the bones to rot. This might indicate the sedimentation rate at the location was relatively low. Indeed some of the (identified) shark bitten bones (the uppermost part of the supraoccipital and the two posterior-most fragments of the ascending process of the maxilla) are part of the vertex, the highest part of the skull, that presumably was exposed the longest to the elements. Detailed descriptions and illustrations of the bite marks are provided in the Supplemental Information file.

DESCRIPTION

Overview. The holotype skull of *Protororqualus wilfriedneesi* is badly damaged and fractured. It includes a partial neurocranium with associated petrotympanic complexes, partial atlas, humerus and ulna. The rostrum includes only the posteromedial portion of both maxillae; nasals and premaxillae were not found and the right periotic is heavily fractured.

Maxilla. The ascending process of the maxilla is long and narrow (Figs. 4–6; Fig. S58); it projects towards the longitudinal axis of the skull but, based on our reconstruction of the skull, the posterior apices of left and right ascending processes of the maxillae do not meet posteriorly but their posterior terminations are very close (Fig. S58). The transverse diameter of the ascending process of the maxilla narrows approaching its almost pointed posterior end. It perfectly fits the most external articular groove found on the interorbital region of the frontal. More anteriorly, the ascending process of the frontal shows a laterally bent dorsal surface and the presence of one dorsal infraorbital foramen.

Frontal. The supraorbital process of the frontal is abruptly depressed from the interorbital region of the frontal (Fig. 7) and it projects laterally. The posterior border projects posterolaterally. The orbit and the anterior border are not preserved. The posterior portion of the base of the supraorbital process of the frontal is located more posteriorly than the anterior end of the supraoccipital in dorsal view (Fig. 4).

A transversely short interorbital region of the frontal is exposed for a short anteroposterior diameter showing articular grooves for the posteromedial elements of the rostrum. A region of the interorbital region of the frontal that lacks these articular grooves is exposed for a few millimeters posteriorly to the posterior end of the ascending process of the maxilla.

The optic canal is localized in the posterior-most portion of the ventral surface of the supraorbital process of the frontal (Fig. 8). It is highly concave and is bordered by anterior and posterior projections of the supraorbital process itself; the anterior border of the optic canal is formed by a crest-like transverse projection crossing the whole ventral surface of the supraorbital process of the frontal.
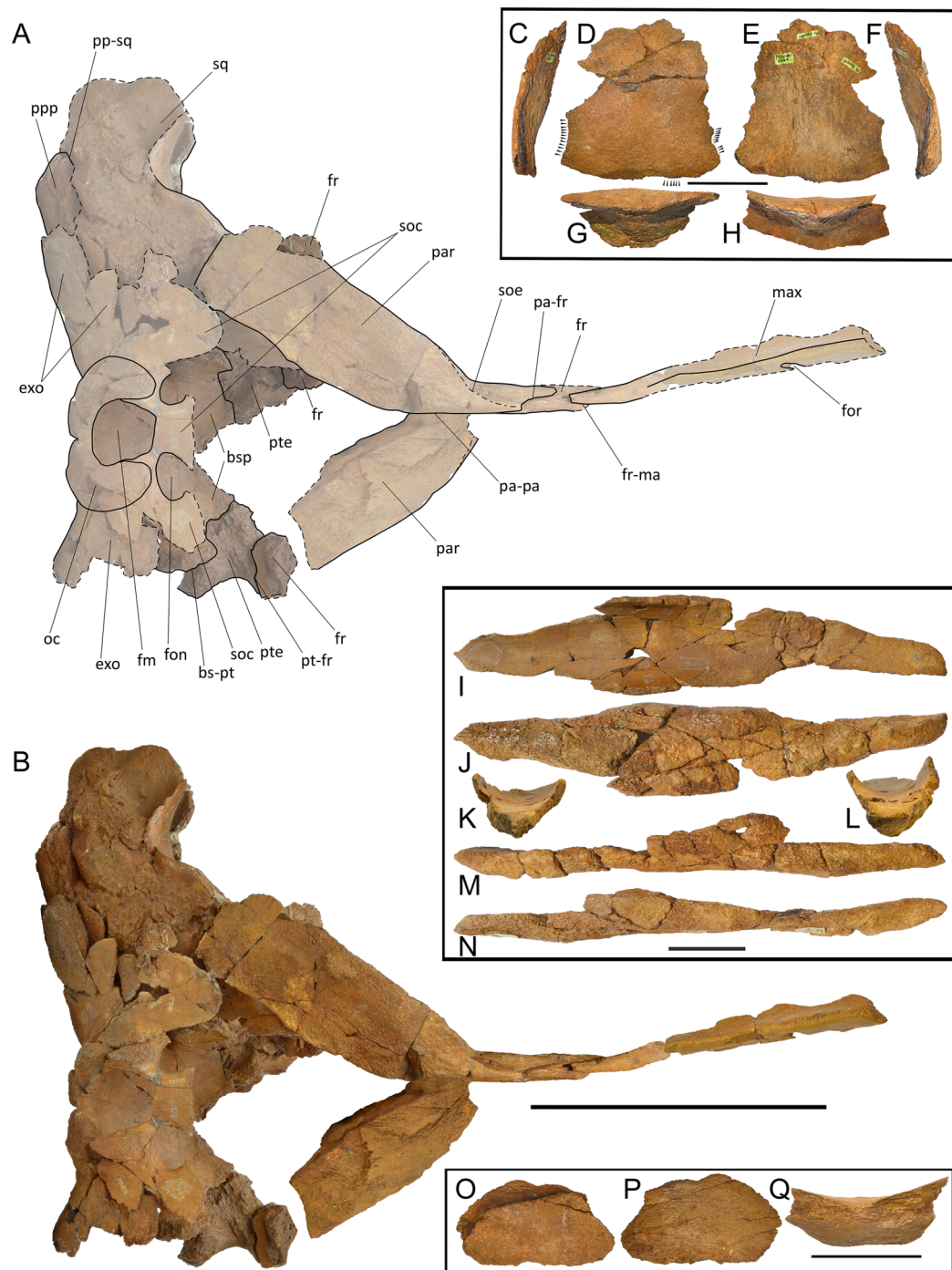
Figure 4 **Holotype skull of *Protororqualus wilfriedneesi* sp. nov. Dorsal view.** Holotype skull of Protororqualus wilfriedneesi in dorsal view with specific anatomical details. (A) Anatomical interpretation of the skull in dorsal view. (B) Photographic representation. (C–H) Fragment of maxilla with bite marks indicated by the arrowheads (a full representation of these shark bites is provided in Figs. S55–S57). (I–N) Vomer in (I) dorsal, (J) ventral, (K) anterior, (L) posterior, (M) left lateral, and (N) right lateral views. (O–Q) fragment of atlas in (O) dorsal, (P) ventral and (Q) lateral views. Scale bar equals 20 cm in (A) and (B), 5 cm in (C–H), (I–N) and (O–Q). See Anatomical abbreviations for explanations of acronyms.
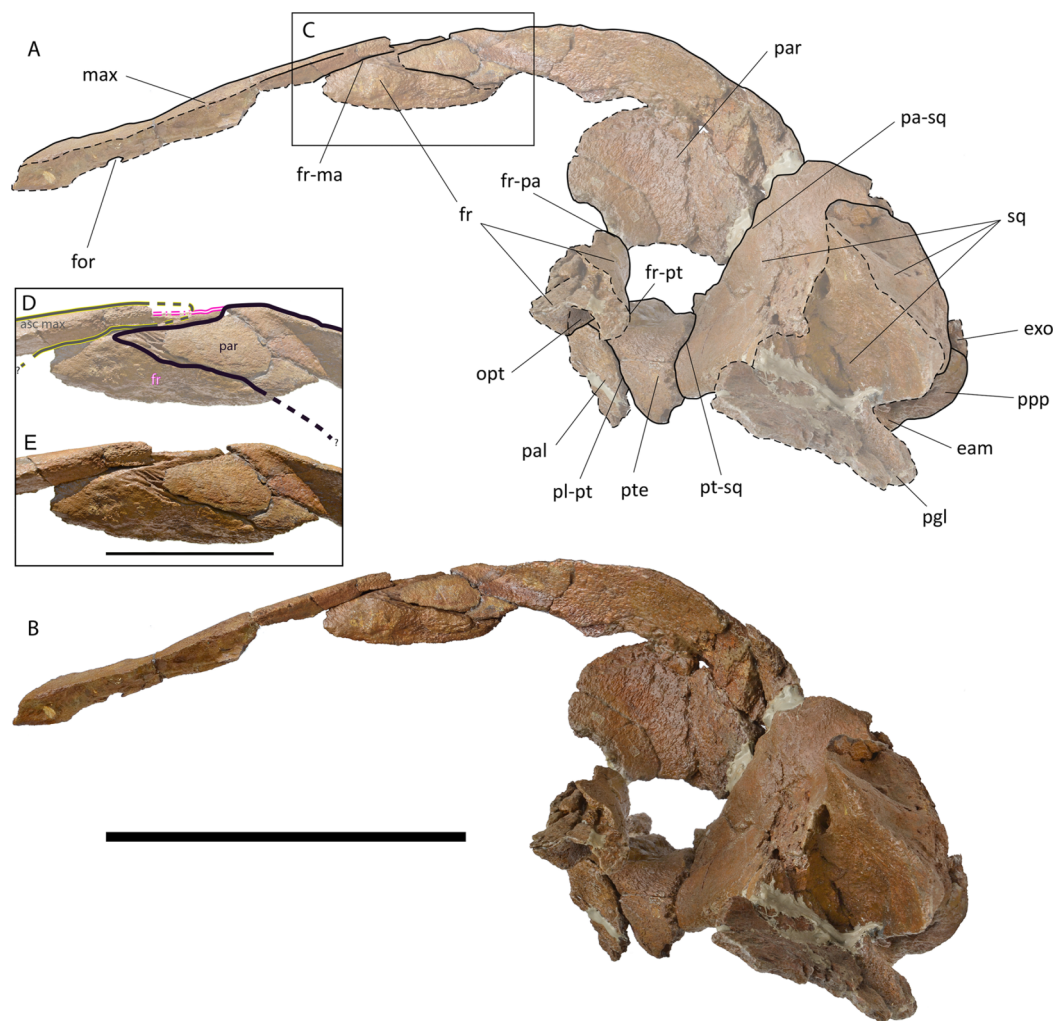
Figure 5 Holotype skull of *Protororqualus wilfriedneesi* sp. nov. Left lateral view. Holotype skull of Protororqualus wilfriedneesi in left lateral view. (A) Anatomical interpretation. (B) Photographic representation. (C) Detail of the articulation of posteromedial elements of the rostrum with frontal and parietal magnificated in the anatomical interpretation in (D) and in the photographic representation in (E) with indication of the fronto-parietal suture (in black). Scale bar equals 20 cm in (A) and (B), and 5 cm in (D) and (E). See Anatomical abbreviations for explanations of acronyms.

Parietal. The parietal is an elongated bone with a dorsoventrally and anteroposteriorly concave external surface. The supraoccipital border of the parietal projects laterally forming the temporal crest that overhangs the temporal fossa and prevents the view of the external surface of the parietal in dorsal view (Fig. 4). Anteriorly and laterally, the parietal superimposes onto the posterior portion of the base of the supraorbital process of the frontal. Dorsally, the parietal is exposed at the skull vertex for *c.* 15 mm anteriorly to the anterior border of the supraoccipital; more anteriorly, the parietal bifurcates and projects anteriorly and ventrally, and interdigitates with the interorbital region of the frontal and the ascending process of the maxilla for a few millimeters (Fig. 4).
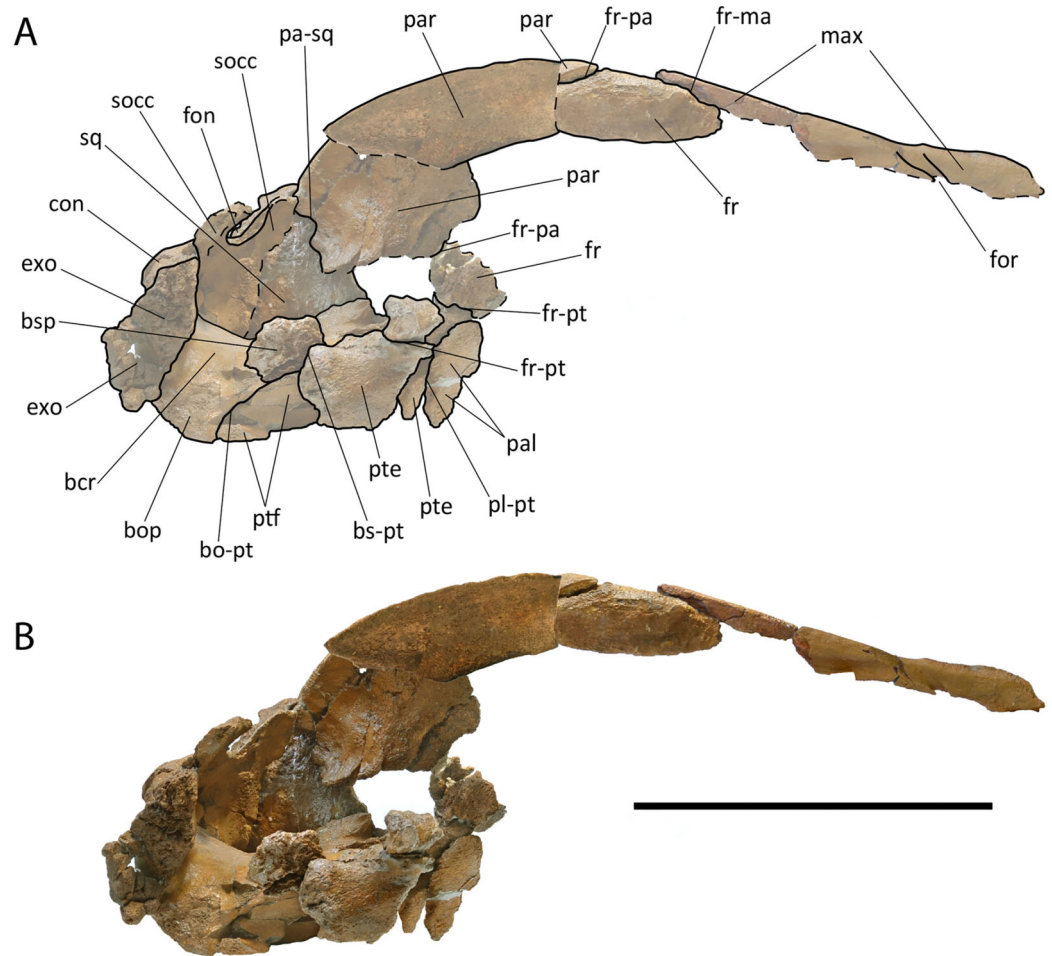
Figure 6 Holotype skull of *Protororqualus wilfriedneesi* sp. nov. Right lateral view. Holotype skull of Protororqualus wilfriedneesi in right lateral view. (A) Anatomical interpretation. (B) Photographic representation. Scale bar equals 20 cm. See Anatomical abbreviations for explanations of acronyms.

Only *c.* 60 mm of the dorsal portion of the parietal-squamosal suture can be observed as the ventral-most portion is missing due to the opening of a hole in the medial wall of the temporal fossa that was caused by post-mortem processes. The observable portion is mainly straight-to-slightly convex. The parietal-squamosal suture starts its path from the presumed parietal-squamosal-alisphenoid contact located anterodorsally to the anterior border of the falciform process of the squamosal (Figs. 5 and 6).

In dorsal view, the supraoccipital border of the parietal is very thick and forms a wide platform for supraoccipital superimposition. Right and left parietals are separated medially by a triangular space that was originally covered by the supraoccipital.

Alisphenoid and temporal fossa. The alisphenoid is not observed in the skull probably because the medial wall of the temporal fossa is badly damaged and there is a large hole in the position that should have been originally occupied by the alisphenoid itself (Fig. 8).
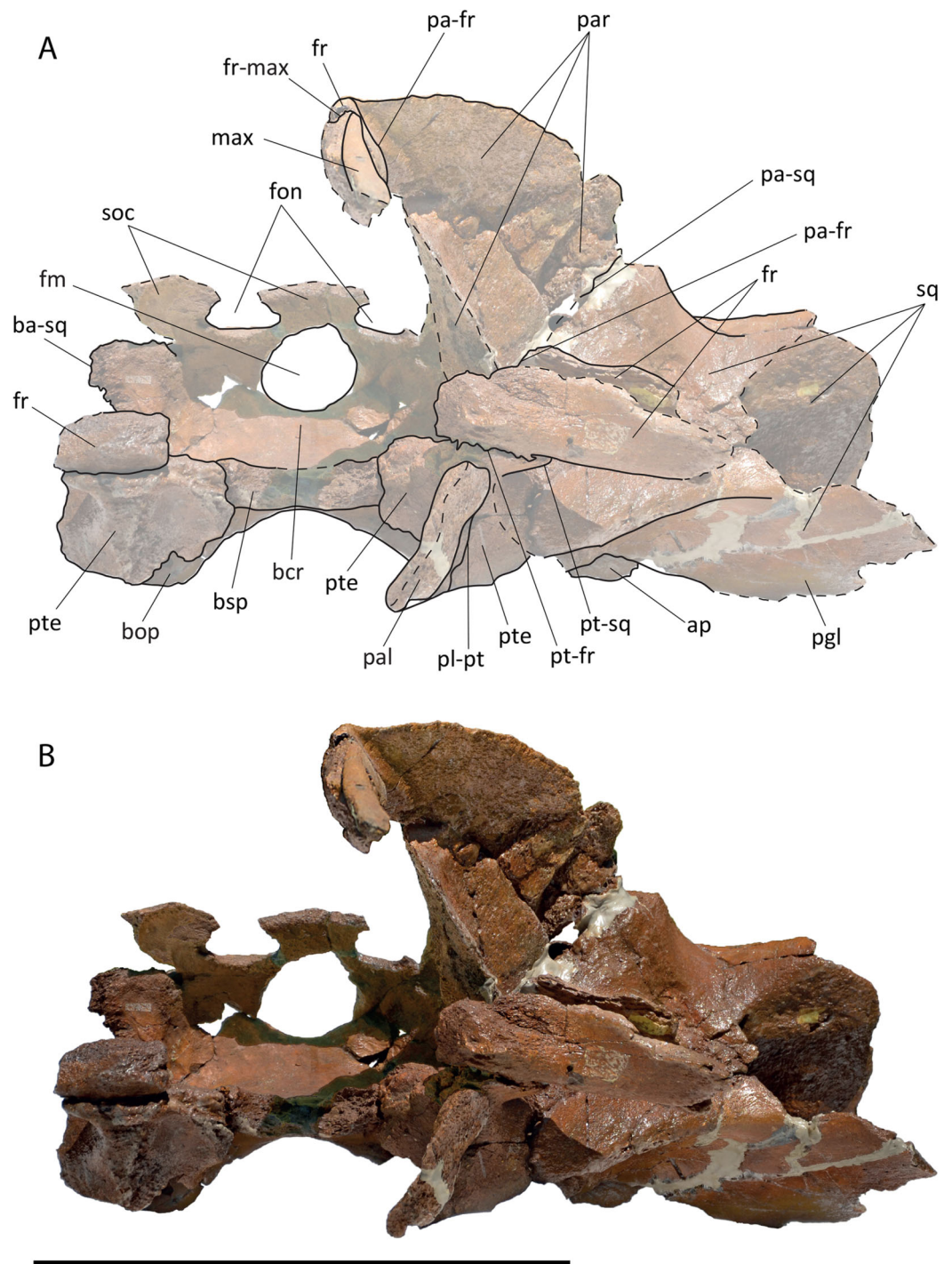
Figure 7 Holotype skull of *Protororqualus wilfriedneesi* sp. nov. Anterior view. Holotype skull of Protororqualus wilfriedneesi in anterior view. (A) Anatomical interpretation. (B) Photographic representation. Scale bar equals 20 cm. See Anatomical abbreviations for explanations of acronyms.
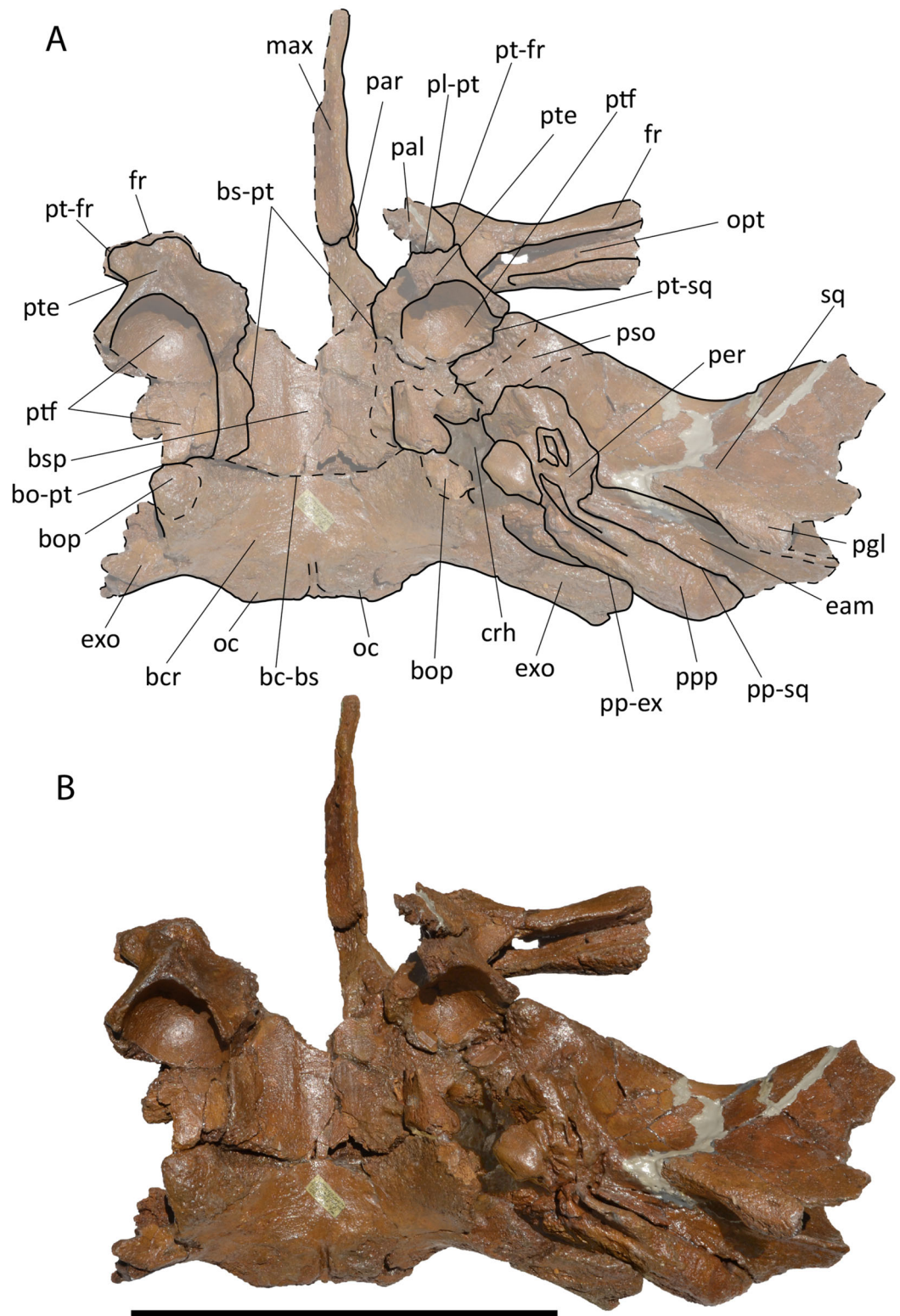
Figure 8 Holotype skull of *Protororqualus wilfriedneesi* sp. nov. Ventral view. Holotype skull of Protororqualus wilfriedneesi in ventral view. (A) Anatomical interpretation. (B) Photographic representation. Scale bar equals 20 cm. See Anatomical abbreviations for explanations of acronyms.

The temporal fossa is comparatively small (with respect to *Protororqualus cuvieri*) because the posterior emergence of the supraorbital process of the frontal is placed more posteriorly thus reducing the anteroposterior diameter of the temporal fossa. Posteriorly to the base of the supraorbital process of the frontal, the pterygoid and the squamosal are in sutural contact being the suture shaped as a straight-to-slightly convex line in lateral view (anterior convexity). It is presumed that the parietal and the alisphenoid were in contact with the pterygoid anterodorsally to the ventral starting point of the parietal-squamosal suture.

Squamosal. The parietal-squamosal suture projects posterodorsally and shows an anterior convexity in its ventral portion (Figs. 5, 6, and 8). The anterior portion of the squamosal forms the posterior part of the medial wall of the temporal fossa and projects posteriorly and laterally. Dorsally, it is bordered by the nuchal crest that projects posteriorly forming a round posterior apex. The squamosal does not bulge into the temporal fossa. The squamosal cleft is present and starts developing from the squamosal-pterygoid suture; it projects posterodorsally and curves lateroventrally *c*. 119 mm from its starting point.

The left zygomatic process of the squamosal is represented only by its anterior apex; this portion shows a flat articular facet for the postorbital corner of the supraorbital process of the frontal. The zygomatic apex is elongated and scarcely curved; it is likely that it projected laterally diverging from the longitudinal axis of the skull as suggested also by the dorsal observation of the lambdoid crest (Fig. 4).

In ventral view, the ventral surface of the squamosal is concave along the anteroposterior and transverse axes (Fig. 8). The anteroventral border of the squamosal is sharply-edged and separates the ventral surface of the bone from the temporal fossa. Part of the postglenoid process is preserved on the left squamosal. It projects posteriorly and ventrally and is posterodorsally bounded by the external acoustic meatus. Its posterior border is rounded. The external acoustic meatus is a highly concave, transversely elongated canal running from the lateral surface of the skull to the petrotympanic complex. This meatus is wide at its distal end and narrow at its medial end. In lateral view, dorsally to the postglenoid process, the lateral surface of the squamosal is concave housing a wide fossa for the neck muscle attachments (Fig. 5).

Supraoccipital. The basal part of the supraoccipital along with the most anterior part of the bone (*c*. 11 cm in lenght) are preserved (Fig. 4). The dorsal surface of the anterior portion is flat to slightly concave transversally, with a very weak bulging along the long axis. Anteriorposteriorly, the dorsal surface is strongly curved. The outline of the supraoccipital border of the parietal, as observed in dorsal view, is a good approximation of the external outline of the supraoccipital itself. As shown in Fig. 4, it may be assumed that the lateral border of the supraoccipital was laterally convex for most of its development. Anteriorly, a lateral concavity was present *c*. 15 mm posteriorly to the anterior end of the supraoccipital. The anterior end of the supraoccipital was short, triangular and pointed resembling *Protororqualus cuvieri* very closely. The posterior
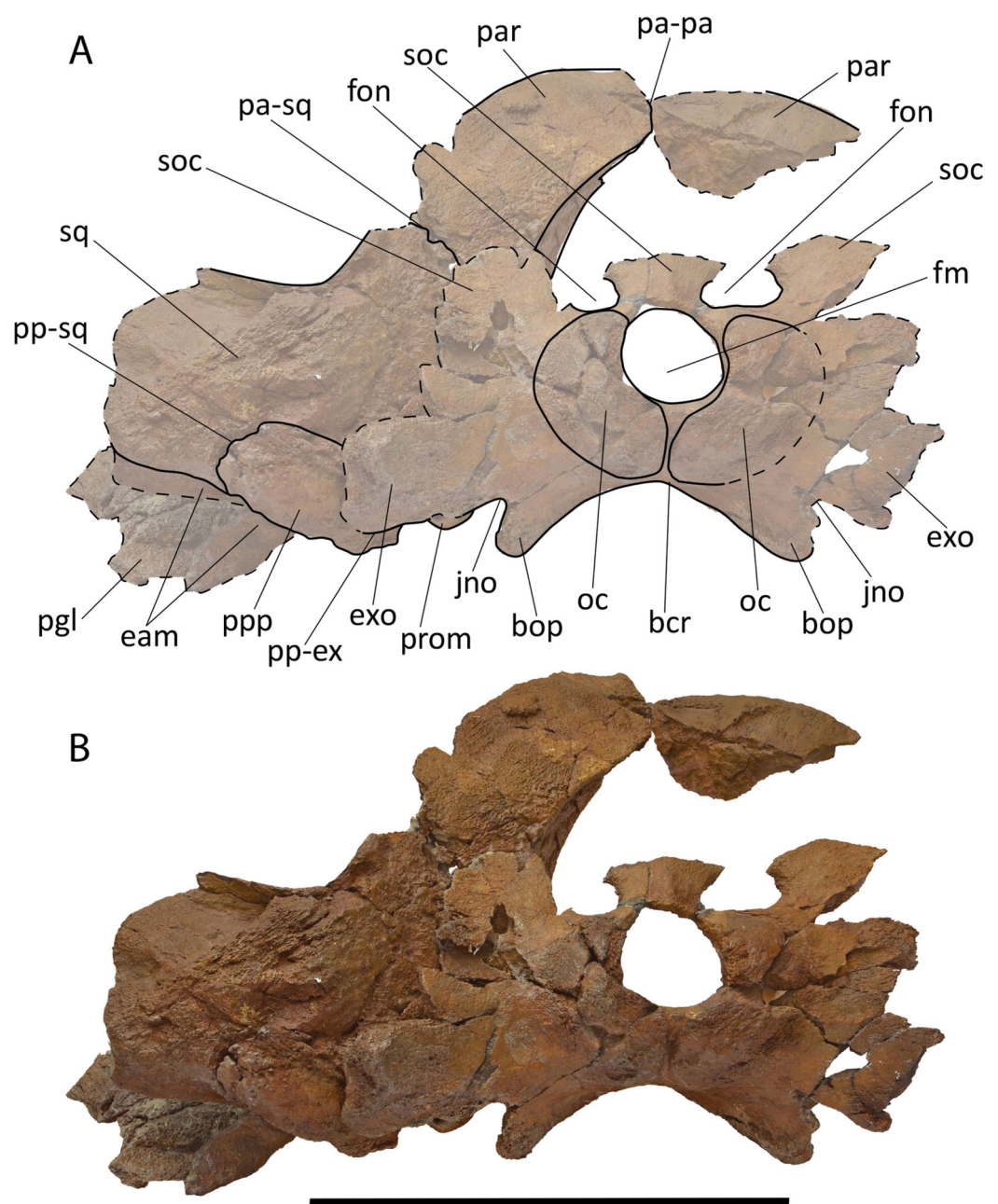
Figure 9 Holotype skull of *Protororqualus wilfriedneesi* sp. nov. Posterior view. Holotype skull of Protororqualus wilfriedneesi in posterior view. (A) Anatomical interpretation. (B) Photographic representation. Scale bar equals 20 cm. See Anatomical abbreviations for explanations of acronyms.

portion of the lateral border of the supraoccipital projects posterolaterally up to the dorsolateral edge of the exoccipital.

Dorsally and laterally to the foramen magnum, there are two wide and elliptical fontanels (Fig. 9). The preserved borders are rather smooth suggesting that the skull was approaching the final phase of closure of the supraoccipital/exoccipital suture (according
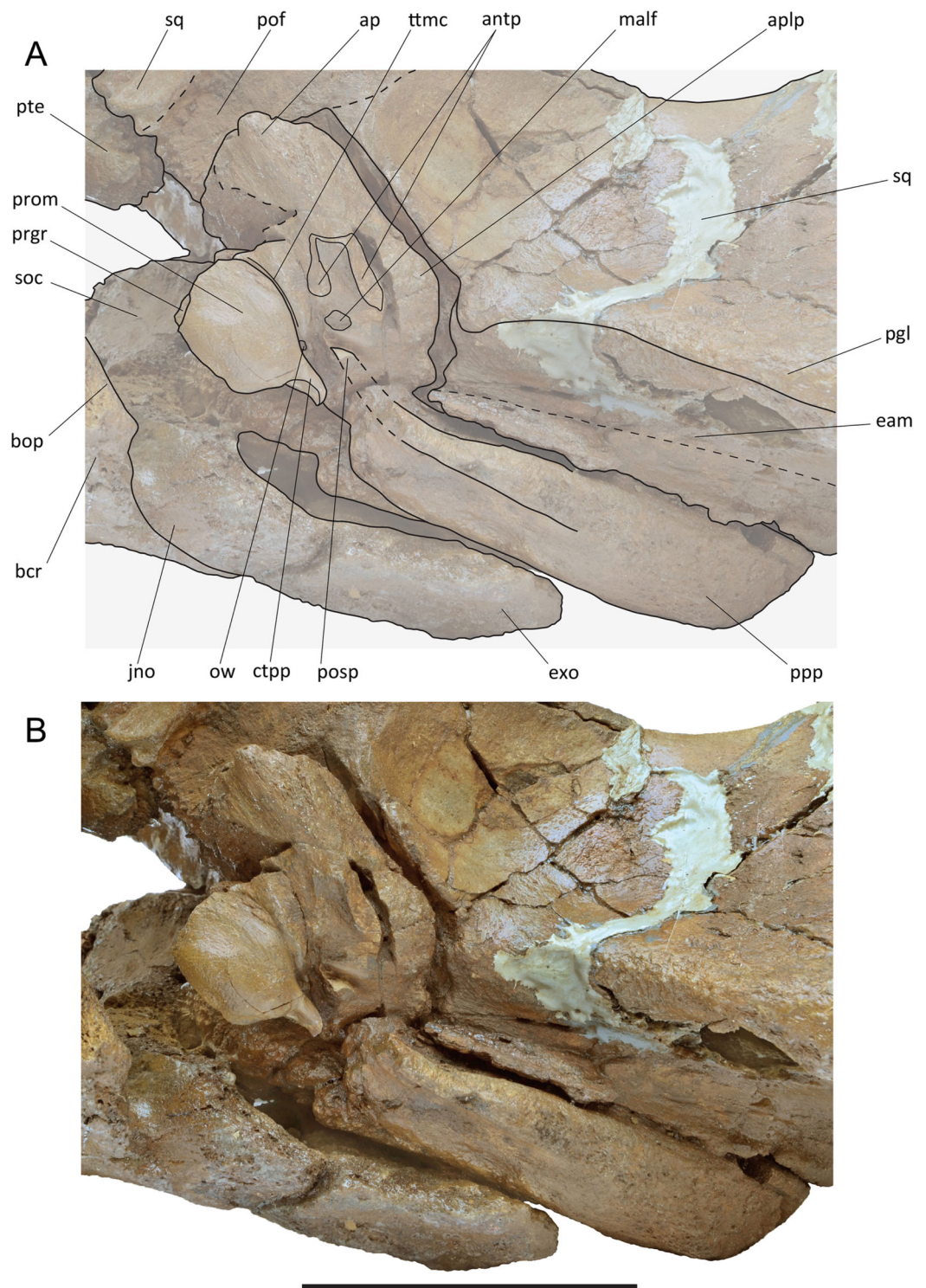
Figure 10 Holotype skull of *Protororqualus wilfriedneesi* sp. nov. Left periotic. Left periotic in articulation with the skull of the holotype skull of Protororqualus wilfriedneesi. (A) Anatomical interpretation. (B) Photographic representation. Scale bar equals 10 cm. See Anatomical abbreviations for explanations of acronyms.

to *Walsh & Berta, 2011*). This phase occurs at different ontogenetic ages in different species of living balaenopteroids but, in any case, in fetuses, neonate or early calf individuals. This suggests that also the holotype of *Protororqualus wilfriedneesi* could be very juvenile. The internal face of the supraoccipital is characterized, posteroventrally, by is a shallow and wide central ridge (*c.* 15 mm thick), ending in an even thicker central bulging (*c.* 20 mm thick). The imprints of the left and right anterior lobes of the brain are visible over the posterior 60 mm on both sides of this ridge, while the anterior 50 mm of the bone fragment show the surface contacting the anterodorsal part of the parietals.

Vertex. The structure of the vertex of *Protororqualus wilfriedneesi* is approximately the same as that of *Protororqualus cuvieri* and includes a triangular and pointed anterior apex of the supraoccipital ending a few mm posteriorly to the frontal-parietal suture; the parietal is exposed at the skull vertex for *c.* 15 mm; no interparietal is observed in the specimen (Fig. 4). The interorbital region of the frontal is transversely narrow and shows dorsal borders that are laterally convex. The posterior ends of the ascending processes of the maxillae approach each other close to the longitudinal axis of the skull but do not meet (Fig. S58); the ascending processes of the maxillae are transversely narrow and to pointed posteriorly and their dorsal surface faces more laterally as soon as they proceed anteriorly. The parietal is interdigitated with the ascending process of the maxilla and with the interorbital region of the frontal in the typical balaenopterid way.

Exoccipital. Part of the left exoccipital is preserved laterally to the foramen magnum (Fig. 9). The exocciptal is lateroventrally thick but transversely flat. It projects posterolaterally and reaches a point located more posteriorly than the articular surface of the occipital condyles. The dorsal edge of the exoccipital forms part of the nuchal crest that is rounded in dorsal view differing from that of *Protororqualus cuvieri* that was triangular.

The foramen magnum is ovoid; its dorsal and ventral borders are straight; its lateral borders are straight and converging dorsally. The occipital condyles are very worn; the dorsal condyloid fossa is highly reduced. The articular surface of the occipital condyles is convex along both the dorsoventral and transverse axes. There are no condyloid foramina. The paroccipital process is anteroposteriorly thick but no paroccipital concavity is observed (Fig. 10).

Pterygoid. Both pterygoids are partially preserved (Figs. 5, 6, and 8). The dorsal lamina enters the temporal fossa and makes contact with parietal and squamosal; more anteriorly, the pterygoid makes contact with parietal and frontal. Its dorsal border is free because there is a hole in the medial wall of the temporal fossa in the position that should be occupied by the alisphenoid. The pterygoid fossa is anteriorly concave; its borders are almost uniformly eroded but a single, small fragment of original border suggests that the ventral lamina (as observed in Balaenidae) was originally absent. The posteromedial portion of the pterygoid fossa is ventrally covered by the lateral projection of the basioccipital crest.
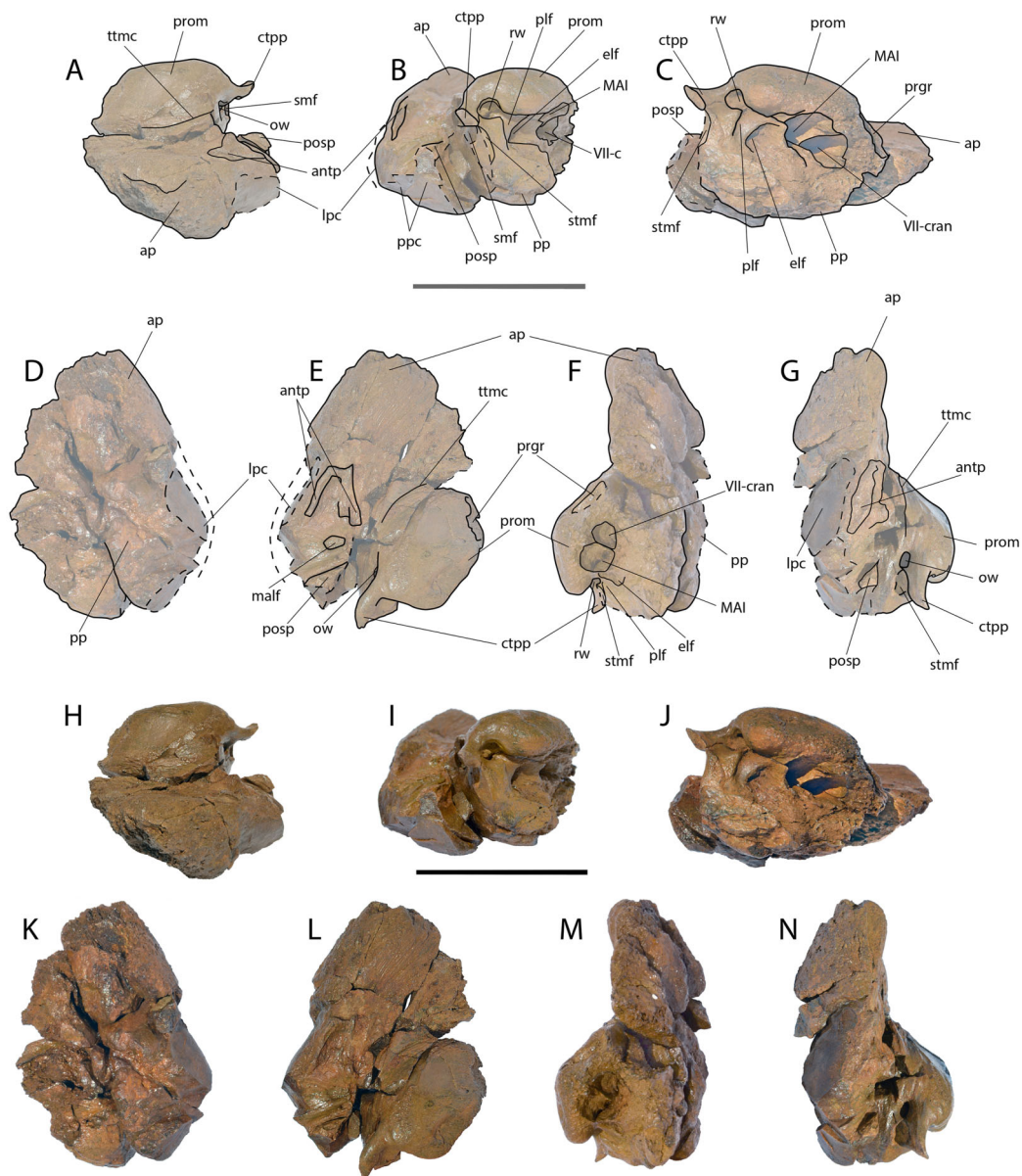
Figure 11 Holotype skull of *Protororqualus wilfriedneesi* sp. nov. Left periotic. Different views of the left periotic of the holotype skull of Protororqualus wilfriedneesi without posterior process and isolated from the skull; (A and H) anterior view; (B and I) posterior view; (C and J) medial view; (D and K) dorsal view; (E and L) ventrolateral view; (F and M) medial view; (G and N) lateral view. Upper sequences represent anatomical interpretations; lower sequences represent photographic representation. Scale bar equals 5 cm. See Anatomical abbreviations for explanations of acronyms.

Basicranium. A fragment of the central portion of the vomer is detached from the skull (Fig. 4D). It is transversely narrow and has a concave mesorostral canal. Its external surface is largely smooth but its external borders are uniformly eroded. A small fragment of the posterolateral corner of the left palatine is still in contact with the anterior border of the pterygoid (Fig. 8). Anteriorly, this small, nearly quadrangular fragment is in contact with

the posterior portion of the base of the supraorbital process of the frontal. Ethmoid and presphenoid are not preserved.

In ventral view, the basisphenoid is wide and short, and dorsally bowed. The basioccipital is wide and anteroposteriorly flat. It becomes convex as far as it approaches the foramen magnum. Below the occipital condyles, the basioccipital crest is tubercle-like and largely flat; in ventral view, the basioccipital crest is oval in shape and its edges are sharp. Transversely, the ventral surface of the basioccipital is concave between the basioccipital crests. The basioccipital crests are elongated parallel to the longitudinal axis of the skull. The posteromedial surface of the basioccipital crest is rough. The jugular notch is included between the medial border of the basioccipital crest and the occipital condyle in posterior view; the jugular notch is small, dorsally concave and transversely narrow. The jugular notch widens approaching the foramen lacerus posterius.

The cranial hiatus is preserved in part. Its anteromedial corner is rounded and narrow and includes a canal running towards the presumed contact of alisphenoid and basioccipital. The medial border is straight and free; the lateral and posterior borders are obliterated by the articulated periotic. The foramen pseudo-ovale is not easy to detect. Only the roof is preserved which is formed by different projections of the squamosal. As it is largely destroyed, it is hard to understand whether it was entirely included within the squamosal or whether it was included between pterygoid and squamosal.

Periotic. The left periotic is still articulated with the skull (Fig. 10) but the right periotic is detached and can be completely described. Measurements are provided in Table S6. In ventral view, the articulated periotic shows that the long posterior process is developed parallel and anteriorly to the external acoustic meatus being separated from it by a sharp, transverse crest. The anterior process is located posteriorly to the pterygoid fossa and occupies the anterolateral and the lateral borders of the hiatus cranicus (Figs. 8 and 10). The anterior process is relatively short (Fig. 11). Its outline is sub-equilaterally triangular, having a width of about 50 mm at its base. Anteriorly the anterior process is obtuse, its top retaining a dorsoventral height of 15 mm and an anteroposterior length of *c.* 20 mm. The anterior pedicle scar is prominent, being 19 mm long and 8 mm wide. It is visible as an oblong oval depression with a sharp rim. The mallear fossa is shallow and ill defined; it has a surface of about 1 cm^2. Anteromedially it is restricted by a small globular protrusion (*c.* 3 mm in diameter). Posteriorly it is separated from the fossa incudis by a weak rounded ridge. The fossa incudis is acute, prominent and about 3 mm deep. The lateral tubercle is weak and obtuse, distinguishable as a slight bulging only.

The pars cochlearis (Fig. 11) is elongated along both the anteroposterior and transverse axes (Table S6). Its anteroventral border gradually merges with the ventral surface of the anterior process. The tensor tympani groove is marked by a crest-like transverse relief. The caudal tympanic process is long, slender and S-shaped. The oval window is elliptical and small; the round window is circular and dorsally confluent with the perilymphatic duct. The endolymphatic foramen is slit-like, dorsoventrally oriented and small. The internal acoustic meatus and the endocranial opening of the facial canal are juxtaposed and coalesced in one big oval foramen, internally separated by a thin, bladelike
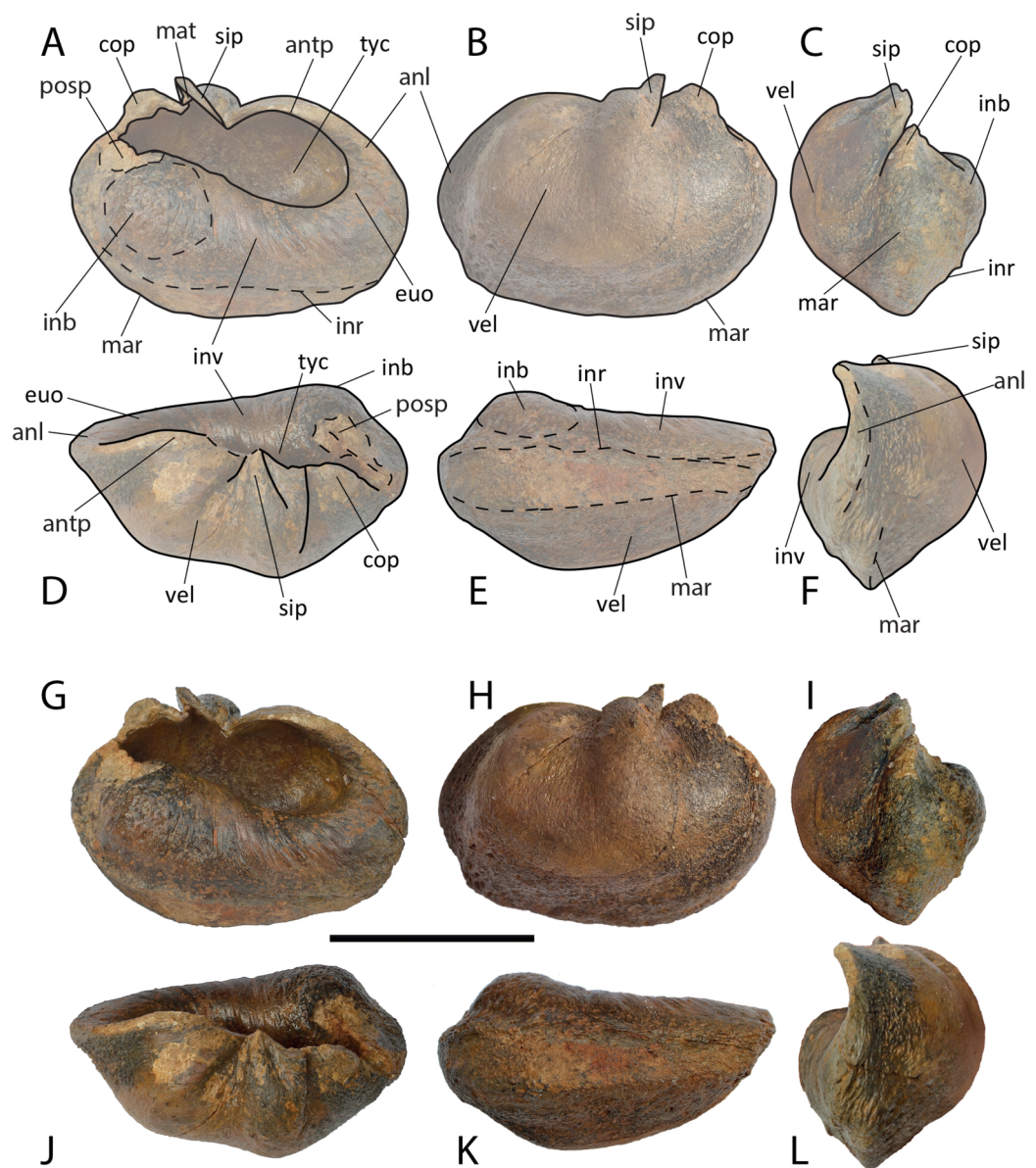
Figure 12 Tympanic bulla of *Protororqualus wilfriedneesi* sp. nov. Left tympanic bulla of Protororqualus wilfriedneesi holotype: photographic representations and anatomical interpretations. (A and G) Medial view; (B and H) lateral view; (C and I) posterior view; (D and J) dorsal view; (E and K) ventral view; (F and L) anterior view. Scale bar equals 5 cm. See Anatomical abbreviations for explanations of acronyms.

crista transversa with sub-millimetric transverse diameter. The promontorial groove appears subdivided into two parts: one located anteroventrally to the endocranial opening of the facial canal and another located posteroventrally to the internal acoustic meatus. The suprameatal area is oriented anteromedially-to-posterolaterally and is anteriorly bordered by a dorsoventral crest that forms the anterior border of the pars cochlearis. The dorsal surface is flat without bulging or depressions.
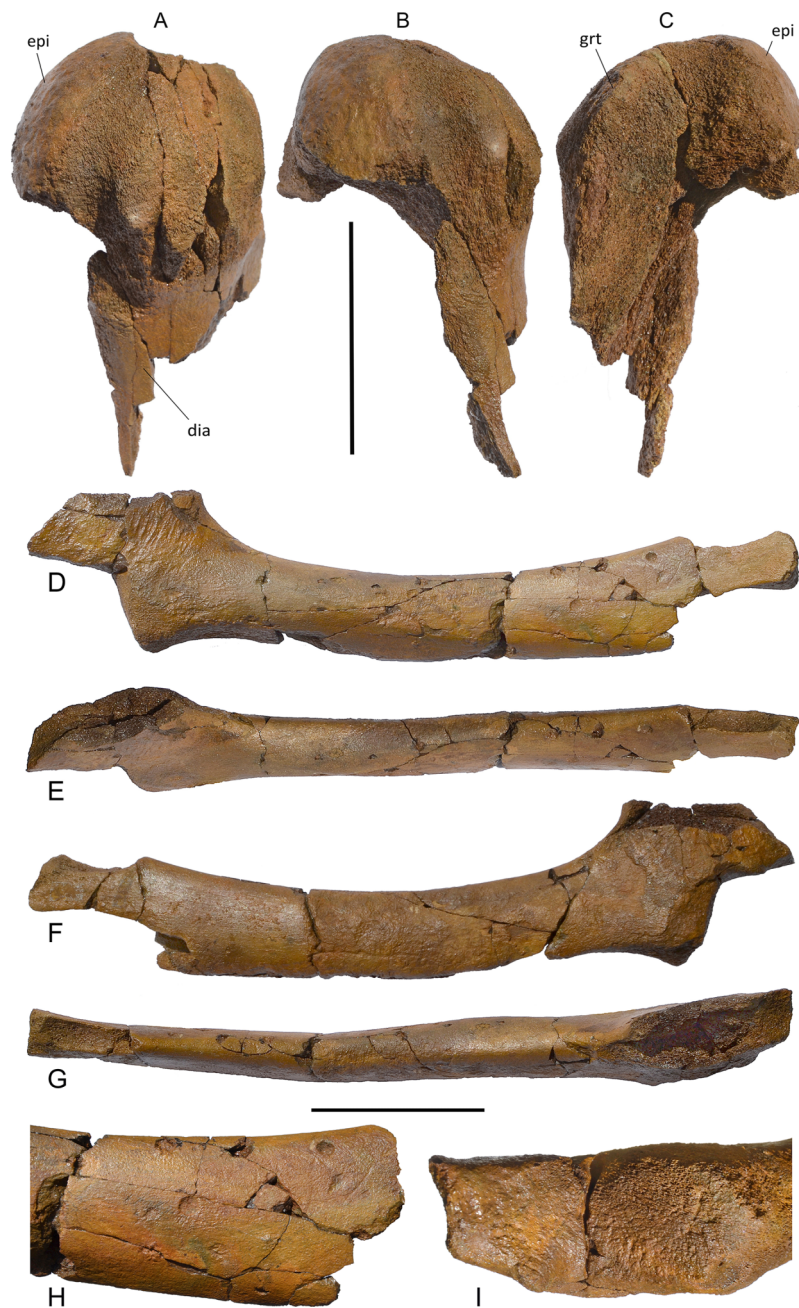
Figure 13 Postcrania of *Protororqualus wilfriedneesi* sp. nov. Postcranial skeleton of *Protororqualus wilfriedneesi* holotype. Humerus in (A) lateral, (B) medial and (C) anterior views. Ulna in (D) lateral, (E) posterior, (F) medial and (G) anterior views, (H) detail of the distal epiphysys of the ulna, (I) detail of proximal epiphysis of the ulna. Scale bar equals 5 cm. See Anatomical abbreviations for explanations of acronyms.

The posterior process is long and robust. It is exposed in the lateral view of the skull as an anteroposteriorly compressed structure located ventrally to the exoccipital and posteriorly to the squamosal (Fig. 10). In ventral view, the ventral surface of the posterior process shows a wide groove for the transit of the facial nerve that is anteriorly bounded
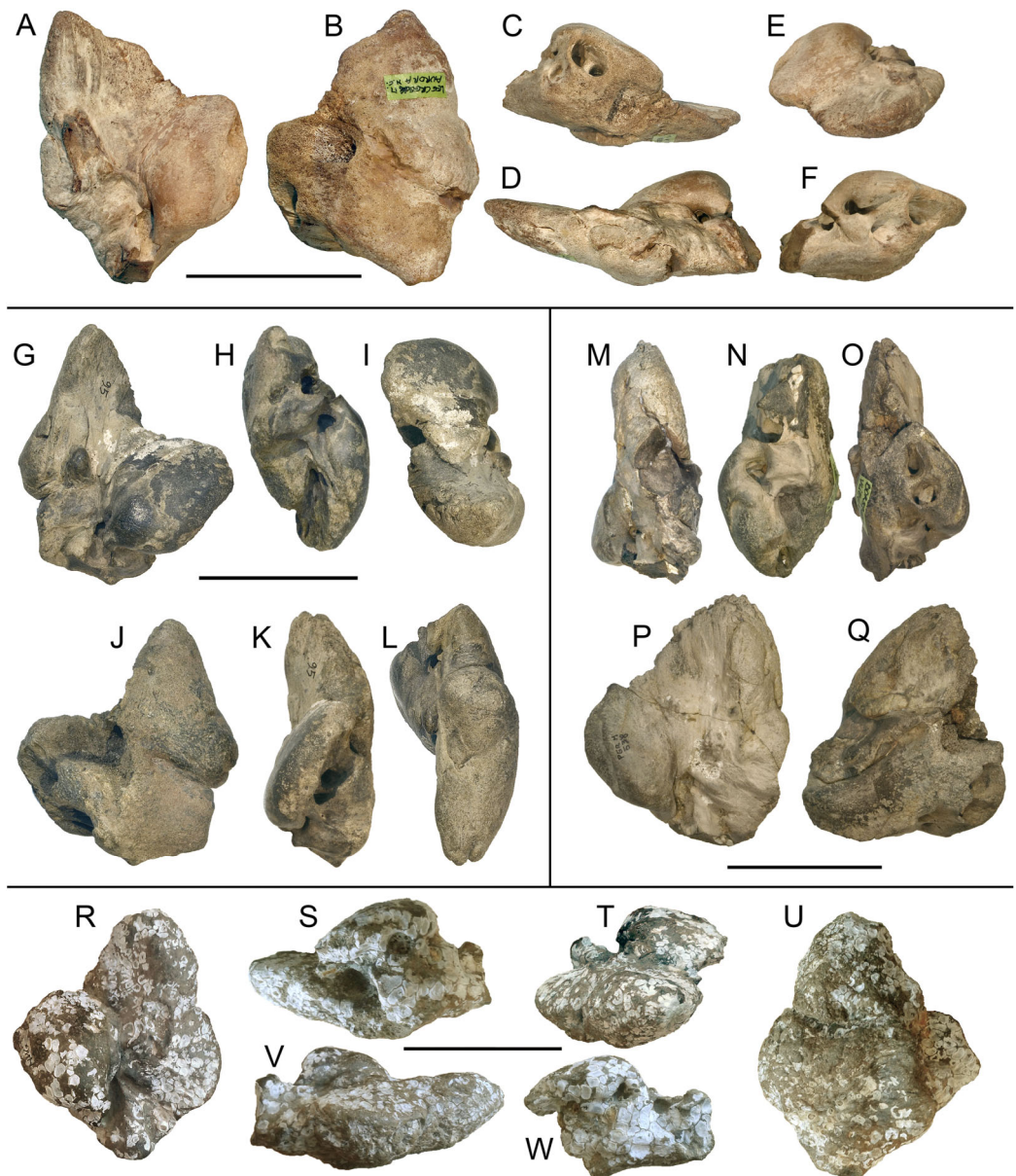
Figure 14 Additional specimens assigned to *Protororqualus wilfriedneesi*. Periotics referred to Protororqualus wilfriedneesi. See text for descriptions. Specimens represented in (A–Q) hold by RBINS; specimen in (R–W) hold by KZGW. (A–F) M 2317. (G–L) M 2318. (M–Q) M 2319. (R–W) No. 23430. Scale bars equal 5 cm.

by a strong, triangular 'anteroventral flange' (*sensu Marx, Bosselaers & Louwye, 2016*). It is *c*. 50 mm wide, *c*. 9 mm long and *c*. 15 mm high. Posteriorly, this groove is defined by a robust and elongated structure. The groove for the facial nerve widens approaching the middle of the length of the posterior process and disappears more posteriorly. In ventral view, the posterior process has a rectangular shape.

Tympanic bulla. In the right tympanic bulla some parts are broken including the sigmoid process and part of the lateral wall but the left tympanic bulla is substantially

complete (Fig. 12). The measurements are provided in Table S7. The bulla has typical balaenopterid characteristics, as discussed by *Bisconti (2010)* and *Ekdale, Berta & Deméré (2011)*, such as a sharply-edged ventral keel, a long anterior lobe and an Eustachian opening anteriorly bordered by a crest-like wall. The sigmoid process is incomplete but, based on its remains, it is expected that it was high; its main surface is oriented transversely with respect to the long axis of the tympanic bulla. The conical process is prominent and with an oval dorsal outline. It is separated from the sigmoid process by a deep incisure. The lateral furrow is not as deep as in the living balaenopterid species (*Ekdale, Berta & Deméré, 2011*) as the anterior lobe (i.e., the anterolateral expansion of *Bisconti, 2010*) is not prominent. In dorsal view, the posterior lobe is shorter than the anterior lobe and lacks the posterior keel as the posterodorsal surface of the tympanic bulla is concave-to-flat. The posterodorsal termination of the ventral keel is at the posterolateral corner of the tympanic bulla. In ventral and posterior view, parallel to the ventral keel there is a slight longitudinal fossa that is dorsomedially bordered by the inferior border of the involucrum. The involucrum is high and thick and surrounds the whole tympanic cavity. A strong inner posterior prominence (that has the shape of a true bulge) is observed at the posteromedial corner of the bulla. The inner posterior prominence gives the medial border of the bulla a concave outline in ventral view. The tympanic cavity is deep and its internal surface is uniformly concave. The anterolateral wall of the tympanic bulla is high and has a rounded dorsal border. The anterior pedicle for the attachment of the bulla to the periotic is located at the dorsal-most portion of the dorsal edge of the anterior lobe; it is broken but its section shows that it was elongated and narrow. The posterior pedicle is also broken.

Humerus. The humerus is badly damaged (Fig. 13). Only a hemispherical articular head is preserved together with a small part of the diaphysys. The anterior border of the diaphysis is laterally concave; the deltopectoral crest cannot be observed due to the bad preservation of the bone. Measurements are in Table S8.

Ulna. The ulna is elongated and slender (Fig. 13). The diaphysis is long and narrow (Table S8) with a uniformly convex anterior border and a uniformly concave posterior border. The distal epiphysis is partially broken. The lateral surface of the diaphysis is almost transversely flat and the medial surface is more convex. The proximal articular facet is small and almost flat with oblique orientation with respect to the long axis of the bone. The outline of the articular facet for the humerus is elliptical. The olecranon is high and shaped as a trapezium in lateral view. Unfortunately, its posterior border is broken. Its dorsal edge terminates proximally with a pointed apex while its ventral border is continuous with the posterior border of the diaphysis.

Referred materials: periotics referred to *Protororqualus wilfriedneesi*
The localities of the discoveries are presented in Fig. S59.

RBINS M2317
Origin. Lee Creek Mine, Aurora, North Carolina, U.S.A.

Stratigraphy. Yorktown Formation (Lower Pliocene: 5–3 Ma; *Ward, 2008*).

Description. Very well preserved right periotic (Fig. 14; Table S8) that is almost identical to the holotype specimen of *Protororqualus wilfriedneesi*. Only the caudal-most part of the caudal tympanic process and the posterior process are missing. Color: off-white to buff. Anterior process relatively thin dorsoventrally (height: *c.* 14 mm) and anteriorly relatively pointed. Anterior process making contact with the pars cochlearis over its entire length. Pars cochlearis ventrally flattened, mediolaterally elongate and anteroposteriorly short (anteroposterior diameter: 34 mm). Round window and perilimphatic foramen confluent. Stapedial muscle fossa mediolaterally short and ventrodorsally high and having an inflated, slightly convex surface, rather than a concave one (height: 10 mm; width: 12 mm). Stylomastoid/lateral-facial-canal wide (width: 9 mm; depth: 5 mm). Caudal tympanic process broken, onset very slender, narrowing to 3.5 mm as preserved. Lateral process small, wide and obtuse. Fossa incudis sharp and well separated but not very deep; mallear fossa weak, shallow and ill defined. Anterior pedicle scar long, wide and prominent (length: 22.2 mm; width: 11.5 mm). Dorsal surface flat and smooth with a small transverse elevation at the level of the lateral process (= onset of the anterior process). The anterior process becomes very thin, blade-like medially (*c.* 4 mm in height). Anterior process and dorsal surface ventrodorsally low (maximum height: *c.* 28 mm). Rather big fossa (hole) anterodorsally to the internal acoustic meatus, separated from the endocranial opening of the facial canal by a thick septum (9 mm wide). Internal acoustic meatus and endocranial opening of the facial canal adjacent, separated by a 3 mm thin septum. Posteroventrally there is the remnant of the promontorial groove, which is srongly eroded. Endolymphatic foramen slit-like. Attachment surface for the posterior process sub-rectangular: (height: 19 mm; width: 10 mm).

RBINS M2318
Origin. Deurganckdok, Antwerp, Belgium.

Stratigraphy. Basal gravel of Kattendijk Sands, post Miocene basal gravel (Lower Pliocene: 5.3–5 Ma; *De Schepper, Head & Louwye, 2009*).

Description. Well preserved right periotic (Fig. 14; Table S8). Only the caudal part of the caudal tympanic process, a small part of the medial border of the anterior process, adjacent to the promontorium, and the posterior process are missing. The lateral border differs slightly from the type specimen, having a slightly more pronounced lateral tuberosity; apart from that this specimen is identical to the holotype specimen. Colour: yellowish to blue-blackish gray. Posterior process missing. Anterior process rather thick (*c.* 25 mm at its base) and anteriorly obtuse. Anterior process making contact with the pars cochlearis over its entire length. Pars cochlearis ventrally flattened, mediolaterally elongate and anteroposteriorly short (anteroposterior diameter: 34 mm). Round window and perilimphatic foramen confluent. Stapedial muscle fossa mediolaterally short and ventrodorsally high and having an inflated, slightly convex surface, rather than a concave

one (height: 13 mm; width: 12 mm). Stylomastoid/lateral-facial-canal wide and deep (width: 8 mm; depth: 7 mm). Caudal tympanic process broken, onset very slender (5 mm). Lateral process somewhat bigger than that of the type specimen; obtuse. Fossa incudis well separated but not very deep; mallear fossa weak, shallow and ill defined. Anterior pedicle scar long, wide and prominent (length: 22.2 mm; width: 13 mm). Dorsal surface quite flat and smooth with a subtle elevation at the level of the lateral process. Anterior process and dorsal surface ventrodorsally low (height: *c*. 32 mm). Big fossa (hole) anterodorsally to the internal acoustic meatus, separated from the endocranial opening of the facial canal by a septum (5 mm wide as preserved; this part of the periotic is damaged). Internal acoustic meatus and endocranial opening of the facial canal adjacent, separated by a 2 mm thin septum. The promontorial groove is hardly visible due to erosion. Endolymphatic foramen slit-like. Attachment surface for the posterior process trapezoidal: (height: 12 mm; width: 15 mm).

RBINS M2319

Origin. Borsbeek, Antwerp Airport tunnel, Belgium.

Stratigraphy. Reworked Lillo Formation (Post-Miocene); the specimen is Pliocene in age (according to *De Schepper, Head & Louwye, 2009*: 5.3–2.6 Ma); judging from color and preservation, we suggest that it may be Zanclean in age.

Description. Well preserved left periotic (Fig. 14; Table S8). The caudal-most part of the caudal tympanic process, the dorsal part of the lateral tuberosity and the posterior process are missing. The preserved part of the lateral tuberosity indicates that this structure might have been a bit more pronounced than in the holotype specimen. Colour: yellowish gray. Posterior process missing. Anterior process anteriorly rather obtuse. Anterior process making contact with the pars cochlearis over its entire length. Pars cochlearis ventrally flattened, mediolaterally elongate and anteroposteriorly short (anteroposterior diameter: 30 mm). Round window and perilymphatic foramen confluent. Stapedial muscle fossa mediolaterally short and ventrodorsally high and having an inflated, slightly convex surface, rather than a concave one (height: 11 mm; width: 11 mm). Stylomastoid/lateral-facial-canal wide and deep (width: 10 mm; depth: 10 mm). Caudal tympanic process broken, onset very slender (5 mm). Fossa incudis prominent, deep and well separated; mallear fossa shallow and rather well defined. Anterior pedicle scar long, wide and prominent (length: 20 mm; width: 13 mm). Dorsal surface more irregular than in the three other specimens and the type specimen; anteromedially slightly depressed. Anterior process and dorsal surface ventrodorsally low (height: *c*. 33 mm). Rather big fossa (hole) anterodorsally to the internal acoustic meatus, separated from the endocranial opening of the facial canal by a strong septum (6 mm wide). Internal acoustic meatus and endocranial opening of the facial canal adjacent, separated by a 2 mm thin septum. Posteroventrally very strong promontorial groove. Endolymphatic foramen slit-like. Attachment surface for the posterior process broken/damaged; sub-triangular: (height: 15 mm; width: 20 mm).
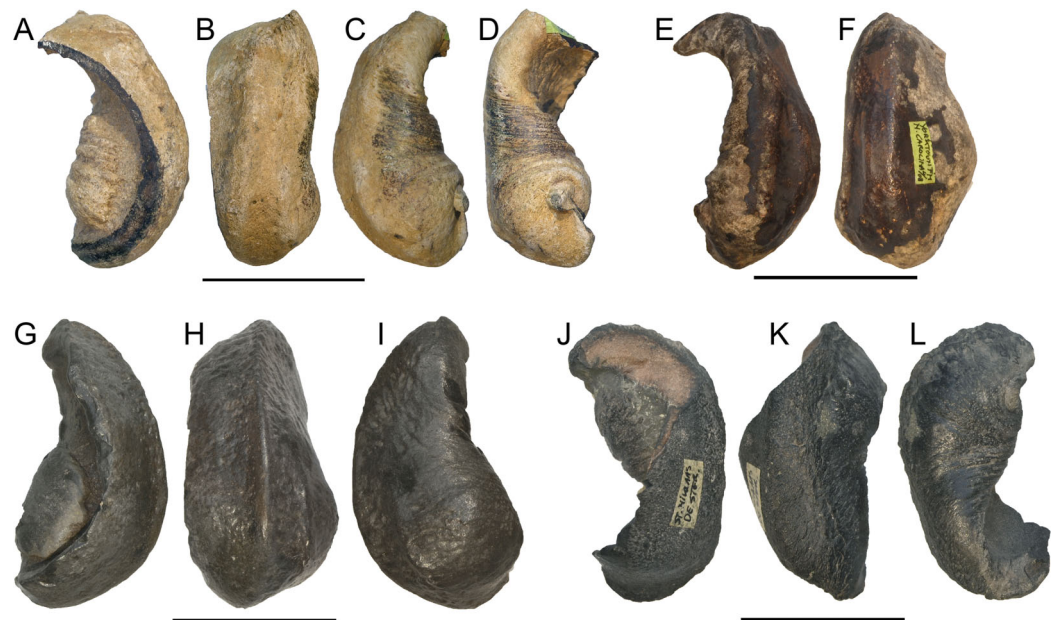
Figure 15 AAdditional specimens assigned to *Protororqualus wilfriedneesi*. Tympanic bullae referred to *Protororqualus wilfriedneesi*. See text for descriptions. All specimens hold by RBINS. (A–D) M 2320. (E–M) M 2321. (G–I) M 2322. (J–L) M 2323. Scale bars equal 5 cm.

NHG 23430

Origin. Specimen trailed from the Western Scheldt River in front of "De Griete", near Terneuzen, The Netherlands.

Stratigraphy. Specimen dragged from the river bed by a fishing vessel; Lower Pliocene (Zanclean: 5.3–3.7 Ma). Stratigraphic information from dragged specimens from the Western Scheldt River are always difficult to retrieve due to a substantial lack of information about the bottom stratigraphy and the exact point of fishing. *Post & Reumer (2016)* reviewed the knowledge about the classical sites of fossil fishing along the Western Scheldt and included also geological profiles and an overview of the fossil content of the relevant sources of sediments for the river bottom. The specimen NHG 23430 comes from a site called 6b by *Post & Reumer (2016)* but, unfortunately, no detailed stratigraphic information is available for it. For this reason, we made a tentative and provisional chronological assessment of the specimen based on color and preservation after extensive comparisons with the Dutch record of mysticete periotics (M. Bosselers, 2004–2018, personal observations) and suggest that it may be coming from the Lower Zanclean Oosterhout Formation that, occasionally, outcrops along the bottom of the Western Scheldt (*Post & Reumer, 2016*).

Description. The specimen is illustrated in Fig. 14 and its measurements are provided in Table S8. Colour: yellowish gray. Posterior process missing. Anterior process relatively short (lenght anterior to the promontorium: 36.4 mm) and anteriorly obtuse. Anterior process making contact with the pars cochlearis over its entire length. Pars

cochlearis ventrally flattened, mediolaterally elongate and anteroposteriorly short (anteroposterior diameter: 32.4 mm). Round window and perilimphatic foramen confluent. Stapedial muscle fossa mediolaterally short and ventrodorsally high and having an inflated, slightly convex surface, rather than a concave one (height: 13 mm; width: 11.2 mm). Stylomastoid/lateral-facial-canal wide and deep (width: 8 mm; depth: 8 mm). Caudal tympanic process broken, onset very slender (8 mm). Lateral process small and very obtuse. Fossa incudis prominent, deep and well separated; mallear fossa weak, shallow and ill defined. Anterior pedicle scar long, wide and prominent (length: 19.6 mm; width: 11.4 mm). Dorsal surface relatively flat with a small elevation at the level of the lateral process; anteromedially slightly depressed. Anterior process and dorsal surface ventrodorsally low (height: *c*. 26 mm). Rather big fossa (hole) anterodorsally to the internal acoustic meatus, separated from the endocranial opening of the facial canal by a septum (3 mm wide at the base; medially broken). Internal acoustic meatus and endocranial opening of the facial canal adjacent, separated by a 3 mm thin septum. Posteroventrally strong promontorial groove. Endolymphatic foramen slit-like. Attachment surface for the posterior process sub-rectangular: (height: 21 mm; widht: 12 mm). The specimen is covered with basal plates of recent barnacles (*Balanus crenatus*). We decided to leave these plates on the fossil, as they indicate/document the ecological circumstances at the river bed where the specimen was trailed.

Referred materials: tympanic bullae referred to *Protororqualus wilfriedneesi*
The localities of the discoveries are presented in Fig. S59.

RBINS M2320
Origin. Fortuinstraat, former fish market, Antwerp city, Belgium (2004/5).

Stratigraphy. Post Miocene basal gravel ('derived Lillo formation'); the specimen is Pliocene in age (according to *De Schepper, Head & Louwye, 2009*: 5.3–2.6 Ma); judging from color and preservation, we suggest that it may be Zanclean in age.

Description. Right tympanic bulla (Fig. 15; Table S9); only the involucrum is preserved, along with the onset of the lateral lobes. Pale yellowish buff color. The anterior lip is missing. Very similar to the type specimen. This bulla shows a prominent main ridge, slightly wider and less pointed than the type; the involucral ridge is marked, forming a slight rim posteriorly and a little offset anteriorly, exactly as in the type. The posterior involucral bulge is slightly rounder and more marked than that of the type. The posterior pedicle is small and circular in section. The involucrum has 3 rather wide striking folds on its posterior bulge and more than 16 finer ones on the middle part, as in the type specimen. The involucrum is a bit swollen at the Eustachian outlet.

RBINS M2321
Origin. North Carolina, U.S.A. (purchased *c*. 1999).
Stratigraphy. River deposit, (Yorktown Formation, Lower Pliocene: 5–3 Ma; *Ward, 2008*).

Description. Left tympanic bulla; the medial half of the bulla is preserved (Fig. 15; Table S9). Colour: speckled buff and gray, ventrally covered by a thin purplish-brown crust. The bulla shows a prominent main ridge, wider and less pointed than the type, anteriorly weakening; the involucral ridge is marked. The posterior involucral bulge is strongly protruding and much more marked than that of the type. The posterior pedicle is small and sub-circular in section. The involucrum has 5–6 rather wide striking folds on its middle part and remnants of finer striae, almost invisible due to erosion. The ventral border has a trapezoidal outline rather than a continuous curve.

RBINS M2322
Origin. North Carolina, U.S.A. (purchased ca. 1999).
Stratigraphy. River deposit, Yorktown Formation (Lower Pliocene: 5–3 Ma; *Ward, 2008*).

Description. Right tympanic bulla; only the involucrum is preserved, along with the onset of the lobes (Fig. 15; Table S9). Colour: neutral to yellowish gray. The anterior lip is damaged. It differs from the type specimen in being more pointed anteriorly. It shows a prominent main ridge, even sharper and more protruding medially than that of the type; The involucral ridge is marked, forming a slight rim posteriorly. The posterior involucral bulge is slightly rounder and protrudes more than that of the type. The involucrum has a few wide folds on the middle part; apart from that the involucrum is almost smooth.

RBINS M2323
Origin. "De Ster", Sint Niklaas, Belgium

Stratigraphy. Post Oligocene basal gravel; middle Miocene-Upper Pliocene (18–2.6 Ma; judging from color and preservation, we suggest that the specimen is Zanclean in age).

Description. Left tympanic bulla; only the involucrum is preserved, along with the anterior part of the lobes; the posteromedial part and the lateral half are missing (Fig. 15; Table S9). Colour: blueish gray to black; internally reddish-brown. It is very similar to the type specimen, except for the main ridge, being wider and less protruding medially than that of the type. The involucral ridge is marked, its posterior rim is more prominent and wider than that of the type, indicating this bulla probably belonged to an old(er) specimen. The posterior involucral bulge is slightly swollen, almost identical to that of the type. The posterior part of the involucrum has a few somewhat irregular wide folds while the middle part has 6 rather strong folds. The anterior lip is a bit shorter than that of the type; ventrally it protrudes more and it is ventrodorsally thicker. The involucrum is a bit swollen at the Eustachian outlet.

Comparisons
The genus *Protororqualus* is characterized by a triangular and acutely pointed anterior border of the supraoccipital with externally concave lateral edges, a character found in no other balaenopterid genus. This is a plesiomorphic character shared with many basal thalassotherian taxa, cetotheriids and eomysticetids. The shape of the supraoccipital may

show different morphologies in different chaeomysticete cetaceans. In Balaenopteridae, a triangular anterior end of the supraoccipital is known in *Protororqualus*, *'Balaenoptera' ryani* and *'Balaenoptera' cortesii* var. *portisi*. The taxonomy of the latter two taxa is still a complicated issue. For this reason, a new project started at the Università degli Studi di Torino (see "Acknowledgment") that is focused on the redescription, phylogenetic analysis and taxonomic revision of *'Balaenoptera' cortesii* var. *portisi* and *'Balaenoptera' acutorostrata cuvieri* so that we expect that clear taxonomic decisions will be made in the next months. A MESQUITE-assisted mapping of this feature (character No. 130 of our character list; see Supplemental Information) reinforced this observation (Fig. S60). *Protororqualus* may be distinguished from the other balaenopterid taxa because its supraoccipital has widely sinuous lateral border (shared also with *'Balaenoptera' cortesi* var. *portisi*) and anterior-most lateral edges that are externally concave. In other balaenopterid taxa the anterior end of the supraoccipital is not acutely pointed; rather, in crown balaenopterids and their closest relatives (e.g., *Norrisanima miocaena*, *'Balaenoptera' siberi*, *Diunatans luctoretemergo*) the anterior edge of the supraoccipital is transversely widened and may be rectangular in dorsal view. This is especially noteworthy for *'Balaenoptera' siberi* that falls outside *Balaenoptera* in some recent works (*Bisconti & Bosselaers, 2016*; *Bisconti, Munsterman & Post, 2019*; *Bisconti et al., 2020*).

A MESQUITE-assisted mapping of this feature (character No. 132 of our character list in Supplemental Information; see Fig. S61) suggests that a transverse enlargement of the supraoccipital is a trend of Balaenopteridae as it may be observed that the supraoccipital is wider in taxa that are closer to the living balaenopterid whales and narrower in early-diverging taxa (such as *Archaebalaenoptera*, *Protororqualus*, *'B.' cortesii* var. *portisi*, *'B.' ryani* etc.). *Nehalaennia devossi* and *'Balaenoptera' bertae* show a supraoccipital whose anterior border is wider than that of the earliest-diverging taxa but narrower than that of crown balaenopterids. The transverse expansion of the anterior border of the supraoccipital in late-diverging balaenopterids seems paralleled by the increase in the transverse distance between the posterior ends of the ascending processes of the maxilla. While these processes are very close in *Protororqualus wilfriedneesi*, Cetotheriidae and some basal thalassotherian taxa (e.g., *Pelocetus*, *'Aglaocetus' patulus* etc.), there is a wide distance between them in crown balaenopterids and their relatives (starting from *Nehalaennia*, *Balaenoptera*, their common ancestor and all the descendants of this ancestor). It is not clear why this transverse expansion occurred in balaenopterid evolution. There could be a correlation with a possible expansion of the brain cavity or with the increase in the transverse width of the mouth that led to the augmentation of the transverse diameter of the gape.

Apart from the supraoccipital, *Protororqualus wilfriedneesi* exhibits another suite of plesiomorphic character states. The periotic, for instance, shows the presence of a promontorial groove (character No. 218 of our character list in Supplemental Information), a character absent in more advanced balaenopterids (including *Norrisanima*, *Balaenoptera*, their common ancestor and all the descendants of this ancestor; see the MESQUITE-assisted map of this character in Fig. S62) but still present in archaic taxa such as *Plesiobalaenoptera* and *Fragilicetus*. Interestingly, the promontorial groove was lost
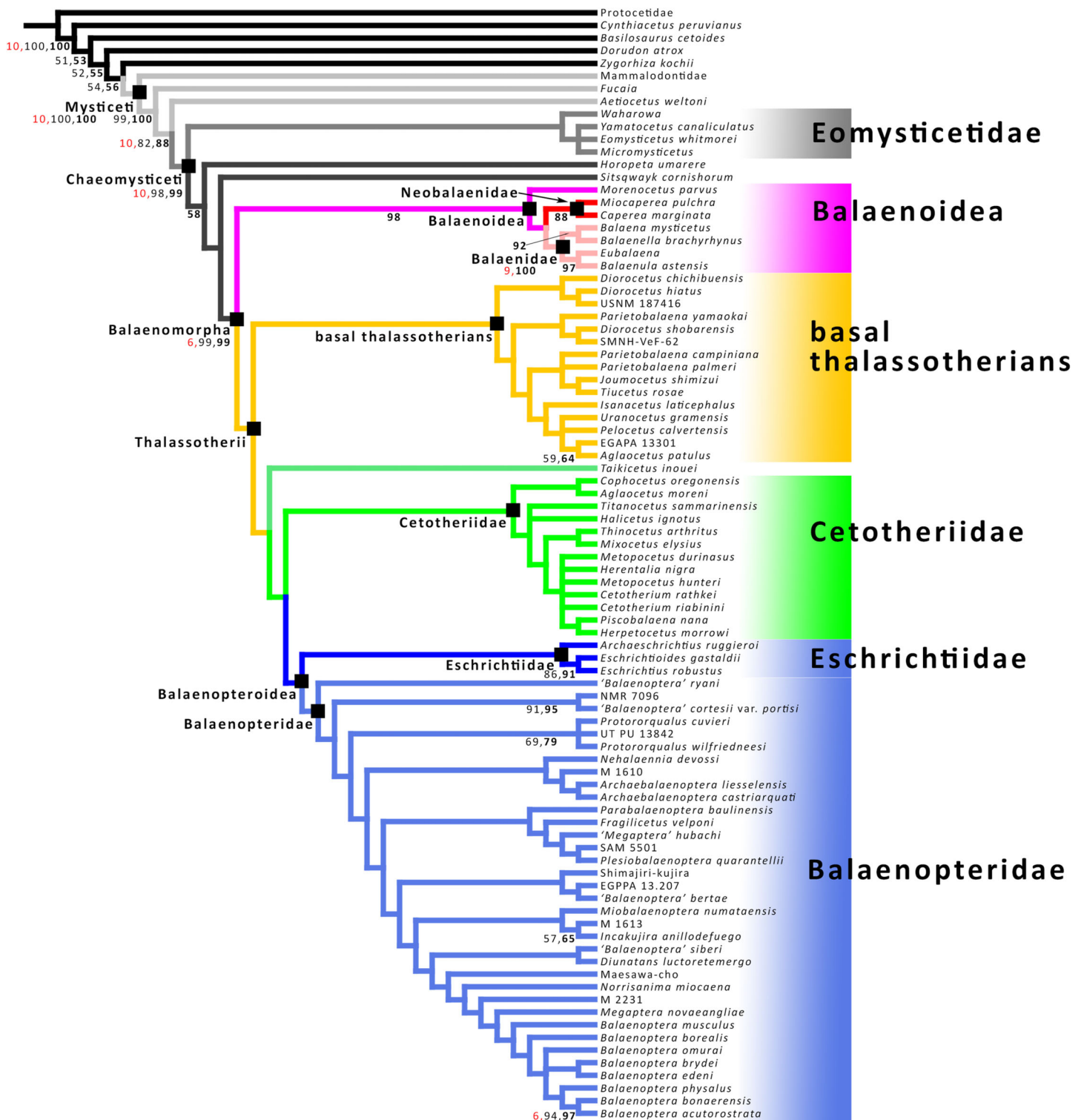
Figure 16 Phylogenetic relationships of Mysticeti. Names at nodes represent named clades. Regular numbers represent bootstrap support values; bold numbers represent support values from symmetric resampling analysis; red numbers represent Bremer support values. Supporting values are provided only for those clades that received 50+% supporting values. Family-rank clades are distinguished by different color patterns, squares and names. See text for methods.

in parallel by the advanced balaenopterids mentioned above, the *'Balaenoptera' cortesii* var. *portisi*, *Eschrichtius robustus* and some of the Oligocene eomysticetid taxa.

The tympanic bulla, on the contrary, shows all the characters of the balaenopterid bulla including a squared anterolateral expansion at the lateral lobe (*sensu Ekdale, Berta & Deméré, 2011*). As shown by a MESQUITE-assisted map of this feature in our preferred tree (character No. 233 of our character list in Supplemental Information), an anterolateral expansion of the tympanic bulla is an apomorphy of Balaenomorpha as it is present in all the family-rank clades described in this group to the exception of a few taxa which should constitute examples of reversals to a primitive condition (Fig. S63). These taxa include basal thalassotherians such as *Parietobalaena palmeri*, *P. campiniana*, *'P.' yamaokai* and *Diorocetus hiatus*.

As demonstrated by a MESQUITE-assisted map of character No. 234 of our character list in Supplemental Information (a character dealing with the relative length of the anterolateral expansion of the tympanic bulla), a long expansion originated independently in Balaenopteridae, members of Clade C of Fig. 16 and some of the other basal thalassotherian taxa (Fig. S64).

Phylogenetic relationships

The results of our phylogenetic analysis are presented in Fig. 16. The Tree Bisection Reconnection algorithm found 32 most parsimonious trees whose strict consensus is shown after examining 5,488,985,590 rearrangements. The best solutions were 1,735 steps in length with a CI of 0.274 and a RI of 0.749 (Fig. 16). The best cladograms resulting from the analysis using implied weights were 1,780 steps in length (0.267 in CI and 0.739 in RI; not shown) and, being less parsimonious than those resulting from the analysis not using the implied weights, were not further considered here.

The main characters of the cladogram in Fig. 16 include the monophyly of Mysticeti, Chaeomysticeti, Balaenomorpha, Balaenoidea, Thalassotherii, Balaenopteroidea, Balaenidae, Neobalaenidae, Cetotheriidae, Eschrichtiidae and Balaenopteridae. Bootstrap, symmetric resampling and Bremer supporting values are reported in Fig. 16 (clades that received less than 50% of bootstrap and symmetric resampling support do not show numbers). The Thalassotherii are subdivided into three main clades, namely basal thalassotherian taxa, Cetotheriidae and Balaenopteroidea. The latter is, then, subdivided into Eschrichtiidae and Balaenopteridae. Noteworthy is the monophyly of the basal thalassotherian taxa that form a family-rank clade that would need a new name. We decided not to name this clade as bootstrap, symmetric resampling and Bremer supporting values are low.

'Balaenoptera' ryani is the basal-most balaenopterid species. Additional basal balaenopterids are *'Balaenoptera' cortesii* var. *portisi* and the *Protororqualus* group including *P. cuvieri*, *P. wilfriedneesi* and the specimen UT PU 13842 that was described in detail by *Caretto (1970)* who assigned it to *Balaenoptera acutorostrata cuvieri*. This taxonomic decision was criticized by *Deméré (1986)* and *Bisconti (2009)* and a new description of this specimen is currently under preparation by one of us (M. Bisconti, 2020, in preparation).
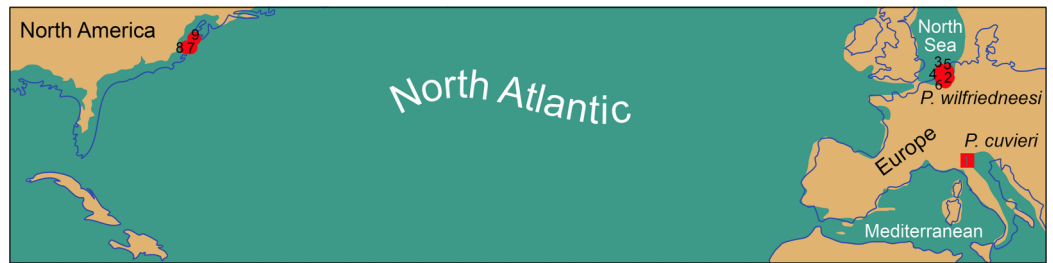
Figure 17 Discovery sites of *Protororqualus* fossils. Map of the North Atlantic, northeastern North America and western Europe and Mediterranean showing the localities of the discovery of Protororqualus fossils. Numbers represent different finds: Protororqualus cuvieri (1, Italy); Protororqualus wilfriedneesi from Belgium (2, RBINS 2315; (3) RBINS 2323; (4) RBINS 2320; (5) RBINS 2318; (6) RBINS 2319) and United States of America (7) RBINS 2317; (8) RBINS 2321; (9), RBINS 2322. The map was realized by us using elements from the following sources: *Prista, Agostinho & Cachão (2015)*, *Neubauer et al. (2015)*, *Rowley et al. (2013)*.

The genus *Protororqualus* is sister to a large clade including *Nehalaennia*, *Archaebalaenoptera*, *Plesiobalaenoptera*, *Parabalaenoptera*, *Fragilicetus*, *Incakujira*, *Miobalaenoptera*, *Norrisanima* and the living *Balaenoptera* and *Megaptera* together with a number of taxa that still have to receive a genus and species name. The subdivision of this large clade is complex as it is formed by: (a) a group including *Nehalaennia* and *Archebalaenoptera*; (b) a group including *Parabalaenoptera*, *Fragilicetus*, *Plesiobalaenoptera* and '*Megaptera' hubachi*; (c) a group including '*Balaenoptera' bertae* and two taxa still unnamed from Italy and Japan; (d) a group including *Miobalaenoptera* and *Incakujira*; (e) the crown balaenopterids (*Balaenoptera* and *Megaptera*) and their stem group including the specimen from Maesawa-cho, '*Balaenoptera' siberi* and *Diunatans luctoretemergo*, and *Norrisanima miocaena*. The specimen RBINS M2231 is from the Early Pliocene of Belgium (see Supplemental Information for a preliminary description of this specimen); it is currently under description by the present authors and, based on our results, represents the sister group of the crown balaenopterid genera.

DISCUSSION

The fossil mysticetes collected in Belgium during the 19th century are still subject of great confusion. *Deméré, Berta & McGowen (2005)* provided a general framework within which it is possible to interpret the taxonomic decisions made by Pierre-Joseph Van Beneden, whose paleontological work on was monumental. Most of the taxonomy provided by Van Beneden is to be rejected today because his methodological approach is not in accordance with contemporary scientific standards (*Deméré, Berta & McGowen, 2005*; *Bosselaers & Post, 2010*; *Steeman, 2010*). This situation led a number of authors to decide to abandon the rich cetacean fossil record of the North Sea previously described by Van Beneden (*Bosselaers & Post, 2010*) or to restrict the study to the periotics only because these anatomical parts have some taxonomic value (*Steeman, 2010*). On the contrary, *Bisconti, Lambert & Bosselaers (2013, 2017)* decided to re-examine the whole record in order to perform piece-by-piece anatomical descriptions for making safer taxonomic decisions without losing information. The new examination is now almost

complete and some outputs are already published such as the taxonomic revisions of *Isocetus* (*Bisconti, Lambert & Bosselaers, 2013*) and *Balaena belgica* (*Bisconti, Lambert & Bosselaers, 2017*). In the present paper, we undertook this same approach based on the affinity shown by the specimen RBINS M 2315 and some of the specimens that were previously assigned to *Burtinopsis* by *Van Beneden (1882)*. As in the other similar revisions, most of the *Burtinopsis* materials come from different localities and represent isolated postcrania that cannot be compared with each other and this makes it impossible to accept the validity of the identifications. In the present case, the specimens can be assigned to several high-rank taxa such as Balaenopteridae gen. et sp. indet., with some individuals that can be assigned to Thalassotherii indet. and Balaenomorpha indet. only. For this reason we decided that *Burtinopsis* is best considered a *nomen dubium*. The only two specimens that closely resemble the current *Protororqualus* specimen (represented by the tympanic bullae RBINS M 702 and M 688) are too incomplete to represent the lectotype or the neotype of a genus, thus, we decided to assign them to the new species *Protororqualus wilfriedneesi* based on the more complete remains of M 2315.

Our analysis of *Protororqualus wilfriedneesi* revealed clear morphological resemblance with *Protororqualus cuvieri* from the Italian Pliocene (*Bisconti, 2007b*) based on the shared triangular and pointed anterior border of the supraoccipital, the shape of the zygomatic process of the squamosal and aspects of the morphology of the tympanic bulla. Our phylogenetic analysis places *P. wilfriedneesi* close to an Italian specimen (*Caretto, 1970*) suggesting that the origin of the genus could be in the Mediterranean and that the invasion of the North Atlantic (as documented by the materials that we referred to *Protororqualus*) and the North Sea was due to a subsequent dispersal event (Fig. 17). Preferential relationships between North Atlantic and Mediterranean were also highlighted by the paleobiogeographic pattern exhibited by *Archaebalaenoptera* (*Bisconti et al., 2020*) even though, in that case, it was the Mediterranean to be invaded by a late-diverging branch of this genus (i.e., *A. castriarquati*). The preferential links between these two basins were also highlighted by analyses of the compositions of the marine mammal faunas all around the world by *Peredo & Uhen (2016a)*. The recent works on the fossil balaenopterids (*Bisconti, Munsterman & Post, 2019*; *Bisconti et al., 2020* and the present work) reinforce their statistical results. However, the scarcely sampled Neogene outcrops of India, Central Asia, The Middle East and Africa (see, e.g., *Govender, 2019a*, *2019b*; *Govender, Bisconti & Chinsamy, 2016*) still represent potential sources of bias as virtually no fossil mysticetes have been collected there (with an interesting exception: *Hampe et al., 2019*); this fact has the potential to obliterate eventual paleobiogeographic connections between the Indian Ocean and the Mediterranean at least during the earlier stages of the Miocene. As the closure of the Eastern seaway stopped the relationships of Mediterranean and the Indian Ocean in the Burdigalian (*Harzhauer et al., 2007*), the strong link between the Mediterranean and the North Atlantic observed for the late Neogene does not suffer from that potential source of bias.

The phylogenetic positions of *Norrisanima miocaena* and *Plesiobalaenoptera quarantellii* suggest that the origin of the *Protororqualus* clade is from the basal Tortonian

(*Bisconti, Munsterman & Post, 2019*). This hypothesis is also supported by the stratigraphic analysis of the branching order of Balaenopteridae provided by *Bisconti, Munsterman & Post (2019)* that placed the origin of the branch leading to *Protororqualus* at *c.* 10 Ma, thus implying the existence of a *c.* 7 million year long ghost lineage. As the Miocene record of Balaenopteridae is patchy and many areas of the world are scarcely sampled for balaenopterid whales, the ghost lineages will not be broken into known sub-units in the next few years but many decades will be necessary to get a comprehensive view of the past balaenopterid diversity.

The hypothesized Tortonian divergence of the *Protororqualus* lineage helps to account for the archaic characters observed in this genus. As demonstrated by a MESQUITE-assisted mapping of character No. 130 on the most parsimonious tree (Fig. S61), the pointed supraoccipital is a plesiomorphic character that has been lost in more advanced balaenopterid whales. The particular shape of the supraorbital process of the frontal, moreover, with its posterior concavity, is morphologically closer to that observed in basal thalassotherian taxa and cetotheriids than to that of balaenopterids. These observations reinforce the hypothesis that *Protororqualus* was an early-diverging balaenopterid ramus retaining primitive characters in the supraoccipital and in the frontal. Rather, the periotic and the tympanic bulla are clearly balaenopterid in shape suggesting that the evolution of the earbone morphology (and, possibly, functions) originated earlier in the evolution of Balaenopteridae.

The discovery of *Protororqualus wilfriedneesi* confirmed the basal position of the *Protororqualus* lineage in the phylogeny of Balaenopteridae. This observation confirms also the early statements in this sense made by *Zeigler, Chan & Barnes (1997)*, *Bisconti (2007a, 2007b)*, *Boessenecker & Fordyce (2015a)* and *Peredo & Uhen (2016b)*. The discovery of *P. wilfriedneesi* certainly allowed for a fine tuning of the phylogenetic relationships of *Protororqualus* generating sounder conclusions based on the new anatomical portions that are now available which include the periotic, the tympanic bulla and details of the vertex and the temporal fossa. Prior to the discovery of *P. wilfriedneesi* these anatomical portions were largely or completely unknown.

We were unable to find any support to some of the sounder results of molecule- or total evidence-based phylogenetic analyses of the mysticetes. In particular, our morphological dataset still supports hypotheses of relationships in which Eschrichtiidae and Balaenopteridae are separate, family-rank taxa that are sister group to each other (vs., e.g., *Árnason et al., 2018*). Moreover, we do not find any evidence of the nesting of *Megaptera novaeangliae* within *Balaenoptera*; rather, we find evidence of monophyly of *Balaenoptera* to the exclusion of *Megaptera novaeangliae*. In this sense, our results strictly conflicts with molecule- and total evidence-based results (e.g., *Árnason et al., 2018*; *May-Collado & Agnarsson, 2006*). We still do not know the reasons of this discrepancy but we think that morphological results better describe the diversity of living balaenopterids and better interpret the character distributions at nodes because of the inclusion of the rich fossil record of this family in the analysis. This is especially true about the evolution of earbone and mandibular morphologies where the morphological results appear most parsimonious with respect to the molecule- or total evidence-results.

Moreover, recent total evidence analyses that found that 'Balaenoptera' cortesii var. portisi is an advanced balaenopterid whale that is more closely related to Eschrichtiidae than to other balaenopterids (*Marx & Kohno, 2016*; *Slater, Goldbogen & Pyenson, 2017*) appears at odds with our results that place it at the base of the balaenopterid tree. Our result finds support in previous works by *Peredo et al. (2018)*, *Peredo & Uhen (2016b)*, *Boessenecker & Fordyce (2015a*, *2015b*, *2016)*, *Bosselaers & Post (2010)*, *Deméré, Berta & McGowen (2005)* and by *Bisconti (2010*, *2007a*, *2007b)*, *Bisconti & Bosselaers (2016)* and *Bisconti, Lambert & Bosselaers (2013)*, *Bisconti, Munsterman & Post (2019)*, *Bisconti et al. (2020)*. Anyway, the discrepancies between molecule-based and morphology-only-based phylogenetic results should be specifically addressed through an ad hoc study in order to understand the reasons of the profoundly different outputs of these two different methodological approaches.

INSTITUTIONAL ABBREVIATIONS

RBINS Royal Belgian Institute of Natural Sciences, Brussels, Belgium
NHG Natuurlijke Historie Genootschap
KZGW Koninklijk Zeeuwsch Genootschap der Natuurwetenschappen
ZM Zeeuws Museum, Middelburg, The Netherlands

ACKNOWLEDGEMENTS

Many thanks are due to the Mark Young (PeerJ Editor) and to Mark D. Uhen, Toshiyuki Kimura and Robert W. Boessenecker for their constructive and thorough reviews that greatly improved the quality and the clarity of this manuscript. Many thanks are due to Patrick Van Puymbroek, who found the bulla RBINS M 2320 from the Fortuinstraat in Antwerp; Jaap Schot, the Skipper of the ZZ10, who dragged NHG 23430; D. Van de Poele, who collected bulla RBINS M 2323; and Mark Bennett who collected the periotic RBINS M 2317 from Lee Creek Mine. The authors wish to thank Annelise Folie, Cecilia Cousin and Alain Dreze, for the access to the RBINS collections and Karina Leynse and Ron Leeuwenburg for the access to the collections of the Zeeuwsch Genootschap at the Zeeuws Museum Middelburg.

Funding

Michelangelo Bisconti's work was funded by two Synthesys 2 grants (Synthesys Project http://www.synthesys.info/), which were financed in 2012 and 2010 by the European Community Research Infrastructure Action under the FP 7 (Projects BE-TAF 3057: Skeletal analysis of archaic mysticetes from Belgium and Progetto BE-TAF 305: Taxonomic revision of fossil balaenopterids from Belgium). Michelangelo Bisconti's current work at the Università degli Studi di Torino is supported by the 2019-UNTODST-0000015 grant that is funded by the Fondazione CRT and a project on the taxonomic revision of mysticetes from Piedmont (Northwestern Italy: assegno di ricerca DD4801). There was no additional external funding received for this study. The funders had no role
in study design, data collection and analysis, decision to publish, or preparation of the manuscript.

Grant Disclosures

The following grant information was disclosed by the authors:
European Community Research Infrastructure Action: FP 7.
Fondazione CRT: 2019-UNTODST-0000015.
Piedmont (Northwestern Italy): DD4801.

Competing Interests

The authors declare that they have no competing interests.

Author Contributions

- Michelangelo Bisconti conceived and designed the experiments, performed the experiments, analyzed the data, prepared figures and/or tables, authored or reviewed drafts of the paper, and approved the final draft.
- Mark E.J. Bosselaers conceived and designed the experiments, performed the experiments, prepared figures and/or tables, authored or reviewed drafts of the paper, and approved the final draft.

Data Availability

Measurements, list of morphological characters and matrix used in the phylogenetic analysis, a list of analyzed taxa, their ages, specimen accession numbers, and repositories are available in the Supplemental Information.

New Species Registration

The following information was supplied regarding the registration of a newly described species:

Publication LSID: urn:lsid:zoobank.org:pub:0E5931ED-C1B7-44D5-BBB4-0A74C9A06A55.

Protororqualus wilfriedneesi sp. nov. LSID: urn:lsid:zoobank.org:act:D125B81C-F7AD-4E3E-8589-4BFBD54D1401.

Supplemental Information

Supplemental information for this article can be found online at http://dx.doi.org/10.7717/peerj.9570#supplemental-information.

REFERENCES

Árnason U, Lammers F, Kumar V, Nilsson MA, Janke A. 2018. Whole-genome sequencing of the blue whale and other rorquals finds signatures for introgressive gene flow. *Science Advances* **4(4)**:eaap9873 DOI 10.1126/sciadv.aap9873.

Bisconti M. 2015. Anatomy of a new cetotheriid genus and species from the Miocene of Herentals, Belgium, and the phylogenetic and paleobiogeographic relationships of Cetotheriidae s.s.

(Mammalia, Cetacea, Mysticeti). *Journal of Systematic Palaeontology* **13(5)**:377–395
DOI 10.1080/14772019.2014.890136.

Bisconti M. 2010. A new balaenopterid whale from the late Miocene of the Stirone River, northern
Italy (Mammalia, Cetacea, Mysticeti). *Journal of Vertebrate Paleontology* **30(3)**:943–958
DOI 10.1080/02724631003762922.

Bisconti M. 2009. Taxonomy and evolution of the Italian Pliocene Mysticeti (Mammalia, Cetacea):
a state of the art. *Bollettino della Società Paleontologica Italiana* **48**:147–156.

Bisconti M. 2007a. A new basal balaenopterid from the Early Pliocene of northern Italy.
Palaeontology **50**:1103–1122.

Bisconti M. 2007b. Taxonomic revision and phylogenetic relationships of the rorqual-like
mysticete from the Pliocene of Mount Pulgnasco, northern Italy (Mammalia, Cetacea,
Mysticeti). *Palaeontographia Italica* **91**:85–108.

Bisconti M, Bosselaers M. 2016. *Fragilicetus velponi*: a new mysticete genus and species and its
implications for the origin of Balaenopteridae (Mammalia, Cetacea, Mysticeti).
Zoological Journal of the Linnean Society **177(2)**:450–474 DOI 10.1111/zoj.12370.

Bisconti M, Francou C. 2014. I cetacei fossili conservati presso il Museo Geologico di
Castell'Arquato (Piacenza). *Museologia Scientifica Memorie* **13**:31–36.

Bisconti M, Lambert O, Bosselaers M. 2017. Revision of *Balaena belgica* reveals a new right whale
species, the possible ancestry of the northern right whale, *Eubalaena glacialis*, and the ages of
divergence for the living right whale species. *PeerJ* **5(17)**:e3464 DOI 10.7717/peerj.3464.

Bisconti M, Lambert O, Bosselaers M. 2013. Taxonomic revision of *Isocetus depawi* (Mammalia,
Cetacea, Mysticeti) and the phylogenetic relationships of archaic 'cetothere' mysticetes.
Palaeontology **56(1)**:95–127 DOI 10.1111/j.1475-4983.2012.01168.x.

Bisconti M, Munsterman DK, Post K. 2019. A new balaenopterid whale from the late Miocene of
the Southern North Sea Basin and the evolution of balaenopterid diversity (Cetacea, Mysticeti).
PeerJ **7(4)**:e6915 DOI 10.7717/peerj.6915.

Bisconti M, Munsterman DK, Fraaije RHB, Bosselaers MEJ, Post K. 2020. A new species of
rorqual whale (Cetacea, Mysticeti, Balaenopteridae) from the Late Miocene of the Southern
North Sea Basin and the role of the North Atlantic in the paleobiogeography of
Archaebalaenoptera. *PeerJ* **7**:e8315 DOI 10.7717/peerj.8315.

Boessenecker RW, Fordyce RE. 2015a. Anatomy, feeding ecology, and ontogeny of a transitional
baleen whale: a new genus and species of Eomysticetidae (Mammalia: Cetacea) from the
Oligocene of New Zealand. *PeerJ* **3(3)**:e1129 DOI 10.7717/peerj.1129.

Boessenecker RW, Fordyce RE. 2015b. A new genus and species of eomysticetid (Cetacea:
Mysticeti) and a reinterpretation of Mauicetus lophocephalus Marples, 1956: transitional baleen
whales from the upper Oligocene of New Zealand. *Zoological Journal of the Linnean Society*
175(3):607–660 DOI 10.1111/zoj.12297.

Boessenecker RW, Fordyce RE. 2016. A new eomysticetid from the Oligocene Kokoamu
Greensand of New Zealand and a review of the Eomysticetidae (Mammalia, Cetacea).
Journal of Systematic Palaeontology **15(6)**:429–469 DOI 10.1080/14772019.2016.1191045.

Bosselaers M, Post K. 2010. A new fossil rorqual (Mammalia, Cetacea, Balaenopteridae) from the
Early Pliocene of the North Sea, with a review of the rorqual species described by Owen and Van
Beneden. *Geodiversitas* **32(2)**:331–363 DOI 10.5252/g2010n2a6.

Brandt JF. 1873. Untersuchungen über die fossilen und subfossilen Cetaceen Europas.
Memoires de l'Academie Imperiale des Sciences, St. Pétersburg **7**:1–54.

Brisson AD. 1762. *Regnum animale in classes IX Distributum, sive synopsis methodica*. Leiden:
Theodorum Haak.

Caretto PG. 1970. La balenottera delle sabbie plioceniche di Valmontasca (Vigliano d'Asti). *Bollettino della Società Paleontologica Italiana* **9**:3–75.

Cortesi G. 1819. *Saggi geologici degli stati di Parma e Piacenza dedicati a sua Maestà la principessa imperiale Maria Luigia arciduchessa d'Austria duchessa di Parma Piacenza uastalla ecc. ecc. ecc..* Piacenza: Dai Torchj del Majno, 166.

Cuscani-Politi P. 1961. Ancora una nuova specie di *Balaenula* pliocenica con considerazioni introduttive su alcuni misticeti dei nostri musei: Accademia dei fisiocritici in Siena. *Sezione Agraria* **8**:3–31.

Cuvier G. 1823. Des baleines fossiles. In: *Recherches sur les ossements fossiles, où l'on rètablit les caractères de plusieurs animaux dont les révolutions du globe ont détruit les espéces*, Vol. 5. Paris: Dufour et D'Ocagne, 309–398.

Deméré TA. 1986. The fossil whale, *Balaenoptera davidsonii* (Cope 1872), with a review of other Neogene species of Balaenoptera (Cetacea: Mysticeti). *Marine Mammal Science* **2(4)**:277–298 DOI 10.1111/j.1748-7692.1986.tb00136.x.

Deméré TA, Berta A, McGowen MR. 2005. The taxonomic and evolutionary history of fossil and modern balaenopteroid mysticetes. *Journal of Mammalian Evolution* **12(1–2)**:99–143 DOI 10.1007/s10914-005-6944-3.

De Schepper S, Head MJ, Louwye S. 2009. Pliocene dinoflagellate cyst stratigraphy, palaeoecology and sequence stratigraphy of the tunnel-canal dock. *Belgium. Geological Magazine* **146(1)**:92–112 DOI 10.1017/S0016756808005438.

Dewaele L, Lambert O, Louwye S. 2018. A late surviving Pliocene seal from high latitudes of the North Atlantic realm: the latest monachine seal on the southern margin of the North Sea. *PeerJ* **6(5968)**:e5734 DOI 10.7717/peerj.5734.

Ekdale EG, Berta A, Deméré TA. 2011. The comparative osteology of the petrotympanic complex (ear region) of extant baleen whales (Cetacea: Mysticeti). *PLOS ONE* **6(6)**:e21311 DOI 10.1371/journal.pone.0021311.

Fordyce RE, De Muizon C. 2001. Evolutionary history of cetaceans: a review. In: Mazin J-M, De Buffrenil V, eds. *Secondary Adaptation of Tetrapods to Life in Water*. Munich: Verlag Dr. Friedrich Pfeil, 169–234.

Gaemers PAM. 1988. The regional distribution of otolith assemblages; correlation of the interregional zonation with the regional lithostratigraphic formations. In: Vinken R, ed. *The Northwest European Tertiary Basin, Geologisches Jahrbuch, Reihe A 100.* Stuttgart: Schweizerbart Science Publishers, 379–389.

Geisler JH, Sanders AE. 2003. Morphological evidence for the phylogeny of Cetacea. *Journal of Mammalian Evolution* **10(1/2)**:23–129 DOI 10.1023/A:1025552007291.

Goloboff PA, Catalano SA. 2016. TNT version 1. 5, including a full implementation of phylogenetic morphometrics. *Cladistics* **32(3)**:231–238 DOI 10.1111/cla.12160.

Govender R. 2019a. Fossil cetaceans from Duinefontein (Koeberg) an early Pliocene site on the Southwestern Cape, South Africa. *Palaeontologia Electronica* **22(1.6a)**:1–21 DOI 10.26879/673.

Govender R. 2019b. Early Pliocene fossil cetaceans from Hondeklip Bay, Namaqualand, South Africa. *Historical Biology* **61(2)**:1–20 DOI 10.1080/08912963.2019.1650273.

Govender R, Bisconti M, Chinsamy A. 2016. A late Miocene-early Pliocene baleen whale assemblage from Langebaanweg, west coast of South Africa (Mammalia, Cetacea, Mysticeti). *Alcheringa: An Australasian Journal of Palaeontology* **40(4)**:542–555 DOI 10.1080/03115518.2016.1159413.

Gray H. 1977. *Anatomy, descriptive and surgical*. New York: Gramercy Books.

Gray JE. 1864. On the Cetacea which have been observed in the seas surrounding the British Islands. *Proceedings of the Scientific Meetings of the Zoological Society of London* **1864**:195–248.

Hampe O, Hairapetian V, Ataabadi MM, Orak Z. 2019. Preliminary report on a late Tortonian/Messinian balaenopterid cetacean (Mammalia, Mysticeti) from Sistan and Baluchestan Province (Iran). *Geopersia* **9**:65–79 DOI 10.22059/geope.2018.258484.648391.

Harzhauer M, Kroh A, Mandic O, Piller WE, Göhlich U, Reuter M, Berning B. 2007. Biogeographic responses to geodynamics: a key study all around the oligo-miocene tethyan aeaway. *Zoologischer Anzeiger* **246**:241–256.

Kellogg R. 1965. A new whalebone whale from the Miocene Calvert Formation. *United States National Museum Bulletin* **247**:1–45.

Kellogg R. 1931. Pelagic mammals from the Temblor Formation of the Kern River Region, California. *Proceedings of the California Academy of Sciences* **19**:217–397.

Kellogg R. 1968. Fossil marine mammals from the Miocene Calvert Formation of Maryland and Virginia. *United States National Museum Bulletin* **247**:103–197.

Laga P, Louwye S, Mostaert F. 2006. Disused neogene and quaternary regional stages from Belgium: bolderian, houthalenian, antwerpian, diestian, deurnian, kasterlian, kattendijkian, scaldisian, poederlian, merksemian and flandrian. *Geologica Belgica* **9**:215–224.

Linneaus C. 1758. *Systema naturae per regna tria Naturae, secundum classes, ordines, genera, species, cum characteribus, differentiis, synonymis, locis*. Stockholm: Holmiae.

Louwye S, Head MJ, De Schepper S. 2004. Dinoflagellate cyst stratigraphy and palaeoecology of the Pliocene in northern Belgium, southern North Sea Basin. *Geological Magazine* **141(3)**:353–378 DOI 10.1017/S0016756804009136.

Maddison W, Maddison D. 2019. MESQUITE: a modular system for evolutionary analysis. *Available at* https://www.mesquiteproject.org/.

Marquet R. 2002. The Neogene Amphineura and Bivalvia (Protobranchia and Pteriomorphia) from Kallo and Doel (Oost-Vlaanderen, Belgium). *Palaeontos* **2**:1–99.

Marquet R. 2005. The Neogene Bivalvia (Heterodonta and Anomalodesmata) and Scaphopoda from Kallo and Doel (Oost-Vlaanderen, Belgium). *Palaeontos* **6**:1–142.

Marquet R, Herman J. 2009. The stratigraphy of the Pliocene in Belgium. *Palaofocus* **2**:1–39.

Marquet R, Landau B. 2006. The gastropod fauna of the Luchtbal Sand Member (Lillo Formation, Zanclean, Early Pliocene) of the Antwerp region (Belgium). *Cainozoic Research* **5**:13–49.

Martìnez-Cáceres M, Lambert O, De Muizon C. 2017. The anatomy and phylogenetic affinities of *Cynthiacetus peruvianus*, a large *Dorudon*-like basilosaurid (Cetacea, Mammalia) from the late Eocene of Peru. *Geodiversitas* **39(1)**:7–163 DOI 10.5252/g2017n1a1.

Marx FG, Post K, Bosselaers M, Munsterman DK. 2019. A large Late Miocene cetotheriid (Cetacea, Mysticeti) from the Netherlands clarifies the status of Tranatocetidae. *PeerJ* **7(Suppl.)**:e6426 DOI 10.7717/peerj.6426.

Marx FG, Bosselaers MEJ, Louwye S. 2016. A new species of Metopocetus (Cetacea, Mysticeti, Cetotheriidae) from the Late Miocene of the Netherlands. *PeerJ* **4(Suppl.)**:e1572 DOI 10.7717/peerj.1572.

Marx FG, Kohno N. 2016. A new Miocene baleen whale from the Peruvian desert. *Royal Society Open Science* **3(10)**:160542 DOI 10.1098/rsos.160542.

May-Collado L, Agnarsson I. 2006. Cytochrome b and Bayesian inference of whale phylogeny. *Molecular Phylogenetics and Evolution* **38(2)**:344–354 DOI 10.1016/j.ympev.2005.09.019.

Mead JG, Fordyce RE. 2009. The therian skull: a lexicon with emphasis on the odontocetes. *Smithsonian Contributions to Zoology* **627(627)**:1–248 DOI 10.5479/si.00810282.627.

Mitchell ED. 1989. A new cetacean from the late Eocene La Meseta Formation, Seymour Island, Antarctic Peninsula. *Canadian Journal of Fisheries and Aquatic Sciences* **46(12)**:2219–2235 DOI 10.1139/f89-273.

Montgelard C, Catzeflis FM, Douzery E. 1997. Phylogenetic relationships of artiodactyls and cetaceans as deduced from the comparison of cytochrome b and 12S rRNA mitochondrial sequences. *Molecular Biology and Evolution* **14(5)**:550–559 DOI 10.1093/oxfordjournals.molbev.a025792.

Neubauer TA, Harzhauser M, Kroh A, Georgopoulou E, Mandic O. 2015. A gastropod-based biogeographic scheme for the European Neogene freshwater systems. *Earth-Science Reviews* **143**:98–116 DOI 10.1016/j.earscirev.2015.01.010.

Nickel R, Schummer A, Seiferle E. 1991. *Trattato di anatomia degli animali domestici.* Vol. 1. Bologna: Edagricole.

Nyst P-HJ. 1835. *Recherches sur les coquilles fossiles de la province d'Anvers.* Bruxelles: Perichon.

Pavšič J, Mikuž V. 1996. The baleen whale (*Balaenoptera acutorostrata cuvierii*) from Miocene beds near Benedikt in Slovenske gorice. *Slovenia Razprave* **37**:86–96.

Peredo CM, Uhen MD. 2016a. Exploration of marine mammal paleogeography in the Northern Hemisphere over the Cenozoic using beta diversity. *Palaeogeography, Palaeoecology, Palaeoclimatology* **449**:227–235 DOI 10.1016/j.palaeo.2016.02.034.

Peredo CM, Uhen MD. 2016b. A new basal Chaeomysticete (Mammalia: Cetacea) from the Oligocene Pysht Formation of Washington, USA. *Papers in Palaeontology* **2016**:1–22.

Peredo CM, Pyenson ND, Marshall CD, Uhen MD. 2018. Tooth loss precedes the origin of baleen in whales. *Current Biology* **28(24)**:3992–4000 DOI 10.1016/j.cub.2018.10.047.

Post K, Reumer J. 2016. History and future of paleontological surveys in the Westerschelde Estuary (Province of Zeeland, the Netherlands). *Deinsea* **16**:1–9.

Prista GA, Agostinho RJ, Cachão MA. 2015. Observing the past to better understand the future: a synthesis of the Neogene climate in Europe and its perspectives on present climate change. *Open Geoscience* **7(1)**:65–83 DOI 10.1515/geo-2015-0007.

Rowley DB, Forte AM, Moucha R, Mitrovica JX, Simmons NA, Grand SP. 2013. Dynamic topography change of the Eastern United States since 3 million years. *Science* **340(6140)**:1560–1563 DOI 10.1126/science.1229180.

Scager DJ, Ahrens H-J, Dieleman FE, van den Hoek Ostende LW, de Vos J, Reumer JWF. 2017. The Kor & Bot collection revisited, with a biostratigraphic interpretation of the Early Pleistocene Oosterschelde Fauna (Oosterschelde Estuary, the Netherlands). *Deinsea* **17**:16–31.

Schaller O. 1999. *Nomenclatura anatomica veterinaria illustrata.* Roma: Delfino Editore.

Slater GJ, Goldbogen JA, Pyenson ND. 2017. Independent evolution of baleen whale gigantism linked to Plio-Pleistocene ocean dynamics. *Proceedings of the Royal Society B: Biological Sciences* **284(1855)**:20170546 DOI 10.1098/rspb.2017.0546.

Steeman ME. 2010. The extinct baleen whale fauna from the Miocene-Pliocene of Belgium and the diagnostic cetacean ear bones. *Journal of Systematic Paleontology* **8(1)**:63–80 DOI 10.1080/14772011003594961.

Strobel P. 1881. *Iconografia comparata delle ossa fossili del gabinetto di storia naturale dell'Università di Parma.* Parma: Libreria Editrice Luigi Battei.

Uhen MD. 2008. New protocetid whales from Alabama and Mississippi, and a new cetacean clade. *Pelagiceti Journal of Vertebrate Paleontology* **28(3)**:589–593 DOI 10.1671/0272-4634(2008)28[589:NPWFAA]2.0.CO;2.

Van Beneden P-J. 1875. Le squelette de la baleine fossile du Musée de Milan. *Bulletin de l'Academie Royale de Sciences du Belgique* **40**:736–758.

Van Beneden P-J. 1882. Description des ossements fossiles des environs d'Anvers. Genres: *Megaptera, Balaenoptera, Burtinopsis, Erpetocetus. Annales du Musée Royal d'Histoire Naturelle de Belgique* **7**:1–90.

Vandenberghe N, Laga P, Steurbaut E, Hardenbol J, Vail PR. 1998. Tertiary sequence stratigraphy at the southern border of the North Sea basin in Belgium. *Society for Sedimentary Geology Special Publication* **60**:119–154.

Vinken R. 1988. The Northwest European tertiary basin. *Geologisches Jahrbuch Reihe A* **100**:1–508.

Walsh BM, Berta A. 2011. Occipital ossification of balaenopteroid mysticetes. *Anatomical Record* **294(3)**:391–398 DOI 10.1002/ar.21340.

Ward LW. 2008. Synthesis of paleontological and stratigraphic investigations at the Lee Creek Mine. *Virginia Museum of Natural History Special Publication* **14**:1958–2007.

Wesselingh FP, Moerdijk PW. 2010. *De fossiele schelpen van de Nederlandse kust.* Leiden: Nederlands Centrum Voor Biodiversiteit Naturalis.

Zeigler CV, Chan GL, Barnes LG. 1997. A new late Miocene balaenopterid whale (Cetacea: Mysticeti), Parabalaenoptera baulinensis, (new genus and species) from the Santa Cruz Mudstone, Point Reyes Peninsula, California. *Proceedings of the California Academy of Sciences* **50**:115–138.